EStatiG: Wearable Haptic Feedback with Multi-Phalanx Electrostatic Brake for Enhanced Object Perception in VR

NICHA VANICHVORANUN*, KAIST, Republic of Korea
HOJEONG LEE*, KAIST, Republic of Korea
SEOYEON KIM†, Seoul National University, Republic of Korea
SANG HO YOON, KAIST, Republic of Korea

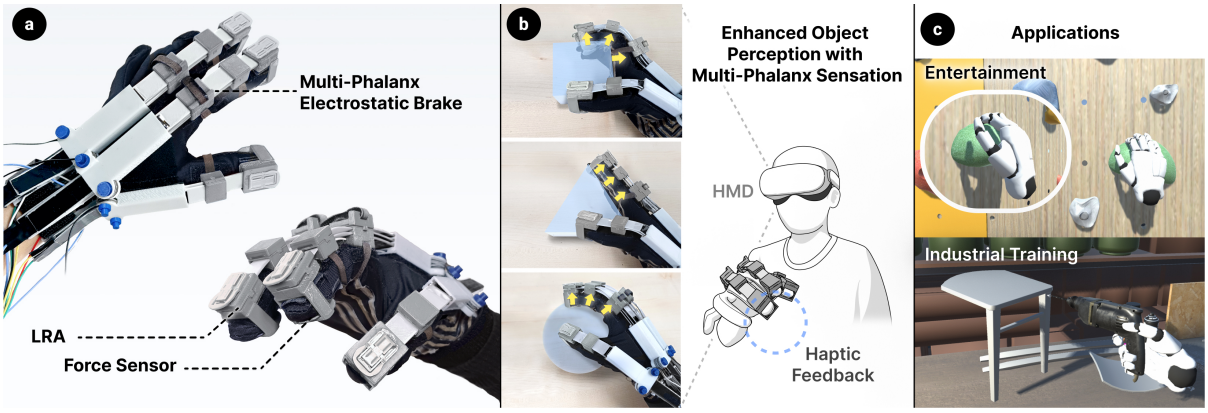

Fig. 1. Overview of EStatiG. (a) We built haptic gloves that provide passive force feedback to multiple phalanges of the finger coupled with vibration motors at the fingertip. We applied force sensors to release actuation upon the force limit. (b) Based on the different shapes of the objects, forces are rendered to each phalanx accordingly upon grasping. (c) EStatiG supports enhanced object perception in VR for immersive experiences.

Haptic gloves have enabled the immersive and realistic sense of interacting with objects in virtual reality (VR) by providing coordinated haptic sensation with visual information. However, previous approaches mainly focused on providing feedback on the fingertips or distal phalanges, with minimal attention paid to the other phalanges. We propose EStatiG, a haptic glove that delivers force feedback over all finger regions from the fingertip to the proximal phalanges. Here, we enrich the perception of object shape during grasping tasks in VR. To do this, we developed the double layer and multi-stacked electrostatic clutches (ES clutches) to form an electrostatic brake (ES brake) for each phalanx. With the lightweight structure (130 grams), we enabled high-resolution force feedback while maintaining wearability and usability. We validated the user

*Both authors contributed equally to this research.
†Work done while the author was at KAIST.

Authors' addresses: Nicha Vanichvoranun, nizetime@kaist.ac.kr, KAIST, 291, Daehak-ro, Yuseong-gu, Daejeon, Republic of Korea, 34141; Hojeong Lee, leeho@kaist.ac.kr, KAIST, 291, Daehak-ro, Yuseong-gu, Daejeon, Republic of Korea, 34141; Seoyeon Kim, kkimseoyeon@snu.ac.kr, Seoul National University, 1, Gwanak-ro, Gwanak-gu, Seoul, Republic of Korea, 08826; Sang Ho Yoon, sangho@kaist.ac.kr, KAIST, 291, Daehak-ro, Yuseong-gu, Daejeon, Republic of Korea, 34141.

ACM 2474-9567/2024/9-ART131
https://doi.org/10.1145/3678567

perception performance when using the proposed device. Our results showed a significant improvement in the perception of phalanx angle positions and the overall experience of realism and immersion when interacting with various object shapes in VR.

CCS Concepts: • **Human-centered computing** → **Haptic devices**; **User studies**; **Virtual reality**.

Additional Key Words and Phrases: Haptics, Virtual Reality, Wearables, Electrostatic Brake

ACM Reference Format:
Nicha Vanichvoranun, Hojeong Lee, Seoyeon Kim, and Sang Ho Yoon. 2024. EStatiG: Wearable Haptic Feedback with Multi-Phalanx Electrostatic Brake for Enhanced Object Perception in VR. *Proc. ACM Interact. Mob. Wearable Ubiquitous Technol.* 8, 3, Article 131 (September 2024), 29 pages. https://doi.org/10.1145/3678567

1 INTRODUCTION

Grasping allows us to perform tasks with objects by seamlessly utilizing the properties of objects, such as shape, size, and stiffness. In Virtual Reality (VR), grasping perception is crucial in providing immersive and realistic experiences that enhance the sense of presence and engagement [7, 10]. In this way, users could perform the same level of manipulation tasks with virtual objects as they would in the physical world. To achieve this, a range of haptic gloves have been developed to provide a realistic sensation of grasping when interacting with virtual objects in various applications from teleoperation [68] to rehabilitation [14]. Some of these gloves offer both vibrotactile and force feedback to produce a grasping sensation.

Haptic gloves recently focused more on delivering force feedback on the fingertip in the area of distal phalanges (DP) [30]. However, researchers often disregarded rendering forces on the intermediate phalanges (IP) and proximal phalanges (PP) due to the hardware complexity and device footprint requirement from motors and pneumatic systems. Attaching many components to the hand easily leads to discomfort during prolonged use and limits natural hand movements. Moreover, it has not been explored whether rendering force feedback on multiple phalanges enhances object perception for VR. Recent work employed a lightweight and a high power-to-size ratio approach using Shape Memory Alloy (SMA) [43], but it lacks responsiveness to support dynamic force feedback. Therefore, it is essential to develop lightweight hardware that renders force feedback for all phalanges.

Recent works have utilized the principle of ES clutch [17, 18], a type of clutch that employs electrical forces to block movement, unlike traditional clutches that often rely on mechanisms like interlocking teeth or magnetic forces. These clutches consist of two high-dielectric layers that create electrostatic adhesion when activated. Then, these clutches act as a brake for the motion between the surfaces. With a given thin and light structure with low power consumption, previous works used ES clutches for exoskeleton [73], haptic gloves [66, 78], and sleeves [31]. However, previous approaches mainly focused on single-node force feedback, which is insufficient to provide a full grasping sensation on the hand.

To promote a full grasping sensation, previous works extended the haptic interface with multi-finger [1] and multi-point [40] force feedback with the hand. Moreover, various haptic rendering approaches have been suggested to overcome the limitations of the hardware. For example, previous works highlighted coordinating the visual content with the haptic feedback during grasping [6, 79]. Some researchers also explored the basic haptic device requirement and perceptual thresholds for carrying out grasping sensations [37, 81]. However, these rendering approaches mostly focused on the fingertips. Therefore, more works are needed to explore the efficient way to utilize full areas within the finger for VR grasping. Furthermore, an understanding of the basic performance of human perception of the object shape, particularly regarding haptic feedback on the finger phalanx area, should be established.

In this work, we propose a wearable haptic feedback approach to deliver force feedback to each phalanx within the finger. We employed PVDF (Polyvinylidene fluoride) instead of PVDF-HFP (Poly(vinylidene fluoride-co-hexafluoropropylene)) used in the previous works [54, 72]. This allows higher flexibility, dielectric constant, and

mechanical strength, which leads to a long activation cycle with a faster release time. In addition, we added linear resonant actuators (LRA) as providing both tactile and kinesthetic feedback can enhance object realism [30]. We carried out a study to investigate the human perception of localizing force at various phalanges. Based on the results, we formed a haptic rendering method for multi-phalanx force feedback. Moreover, we conducted a user study to evaluate our haptic glove performance for identifying phalanx angle positions and realism assessment during grasping tasks. Our work showed a potential to enhance the performance and experience of a conventional single-node force feedback-based haptic feedback approach.

Our contributions are as follows:

- A novel design of multi-phalanx electrostatic brake to enrich the object perception of virtual objects;
- A formation of the haptic rendering conditions and algorithm to operate multi-phalanx electrostatic brake effectively and efficiently;
- Analysis of technical evaluations and user studies to explore the impact of force rendering on the object perception experiences; and
- Example applications demonstrating the enhanced haptic experiences with the proposed multi-phalanx electrostatic brake.

2 RELATED WORK

2.1 Haptic interface for shape rendering on hands in VR

Prior works proposed various haptic feedback approaches to render the shape of VR objects. Here, researchers focused on simulating the skin sensation by creating a sense of touch/contact through skin stretching, compressing, vibrating, and poking [11, 23, 69]. These works employed a mobile haptic feedback platform operated with small motors and a linkage mechanism to stimulate the fingertip. Moreover, other works employed linear resonant actuators (LRAs) [51] and pneumatic pin arrays [59, 71] to enhance cutaneous sensation with vibration and physical displacement with wearable form factor. Although these methods supported numerous sensations of VR objects' shape and texture [34], they cannot align the grasping sensation with VR contexts due to a lack of kinesthetic feedback.

Force feedback or kinesthetic feedback devices have been suggested to restrict or move the hand (or fingers) to render shape during grasping [70]. Early kinesthetic haptic feedback devices were primarily stationary form factors that required a large physical footprint but supported a full 6-DOF control with 3-DOF force feedback [19, 60, 64]. For force feedback rendering research, these devices have been used to generate realistic and high-fidelity haptic feedback with 3D objects [15]. With the advancement of hardware components, researchers started to adopt the force feedback to smaller form factors while meeting minimal force feedback requirements.

Researchers started to develop diverse haptic interfaces for shape rendering with compact and portable form factors including handhelds and wearables. Prior works suggested handheld controllers with integrating pin-based display for 2.5D shape rendering [80], a spinning wheel to render textures [76], combining mechanical brake and voice coil actuators for simulating weight and grasping [13], and expandable rings for grasping [25]. Although these devices were ungrounded, they still required users to hold or be in contact with a controller which prevents natural hand interactions.

To this end, wearable form factors like gloves or wristbands have been suggested to support realistic haptic feedback sensation while allowing natural hand interactions [16, 46, 62]. By directly applying haptic feedback to one's hand, these devices enable realistic and immersive user experience with VR objects. In general, wearable haptic were equipped with actuators and force feedback mechanisms distributed across the fingers [8], palm [35], and wrists [48] to promote natural grasping and manipulating sensation in VR. In our work, we further extend the capability of the wearable haptic interface to promote grasping sensation with a novel kinesthetic force feedback.

2.2 Whole-Hand Haptic Feedback with Wearables

The hand has been highlighted as a main body part to apply diverse forms of wearable haptic feedback to promote enhanced object perception [67] and task performance [22, 39, 74]. For object perception, previous works included kinesthetic haptic feedback as a main feedback method [75] since force is an essential element for the human to acquire shape perception [55]. Kinesthetic feedback generally comprises active and passive actuations. Here, the active force feedback provides active motion and resistance force, while the passive approach only offers resistance force like braking. Although haptic gloves with active actuations using cable-driven [27, 56], tendon-driven [3], pneumatic pump [16], shape memory alloy [43] and twisted-string actuator (TSA) [33] supported realistic force rendering, they exhibit significant drawbacks due to the required power consumption, hardware complexity, and large footprint.

Hence, recent works have focused on implementing compact and highly efficient passive force feedback by supporting only braking forces. Passive force feedback has advantages over the active approach in terms of fewer hardware requirements and a better energy efficiency. Previous works utilized magnetorheological (MR) fluid [4, 77], cable-locking [28, 45], pneumatic jamming [12], eddy-current [20], pawl & ratchet [44], and electrostatic adhesion [30] to resist motion from body parts utilizing various mechanisms. Still, these works support kinesthetic feedback in a single-node fashion. For example, braking force was transferred to either DP, IP, or PP for haptic gloves [52]. Our work aligns with ongoing passive kinesthetic force feedback, where we mainly utilize a braking mechanism for efficient operation. Then, we also enable multi-phalanx force feedback in each fingertip and further propose how to render passive force feedback to multi-phalanx configuration to enhance object perception.

2.3 Electrostatic Clutch/Brake Applications in HCI

ES clutch has been suggested with the advantages of enabling passive force feedback in thin layers and lightweight form factors while maintaining performance reliability [18]. Previous works applied various operating mechanisms and designs to employ electrostatic adhesion in wearable form factors. These include clutch with simple moving strips [29], rubber-spring [17], stretchable textile with moving strip [31], liquid-metal surface [47], all-fabric type [53], and spring-attached pulley [78]. These approaches achieved seamless integration with wearables, enhanced user comfort, and created high-force density.

With these advantages, HCI researchers have started to employ and utilize ES clutches/brakes for interaction purposes. Researchers initially utilized electrostatic adhesion to improve the grasping performance in VR [30, 72]. Here, the authors successfully demonstrated the improvement of grasping performance by minimizing finger-object generation using a clutch along with vibration. Subsequent work expanded the scope of applying ES brake to whole-body garments level [73]. Moreover, the electrostatic adhesion used in the ES brake was also utilized to stimulate variable friction of surfaces for enhanced interactions [2, 42]. In this work, we further expand the capability of the electrostatic braking mechanism by minimizing the footprint while maintaining the amount of force feedback with a multi-layer configuration as well as rapid release time upon deactivation of electrostatic adhesion.

3 ESTATIG OPERATING PRINCIPLE

In this section, we explain the working principle of EStatiG and the basic performance of force rendered by the proposed configuration. An ES clutch forms a braking mechanism that utilizes the friction between two or more components generated by electrostatic adhesion. Here, the ES clutch mainly consists of (1) conductive layers, where one is fixed, and the other layer is attached to the sliding components, and 2) dielectric layer (PVDF), a thin insulating layer that separates the electrodes. An electrostatic attraction occurs between the conductive layers if a relatively high voltage is applied (>200 V).

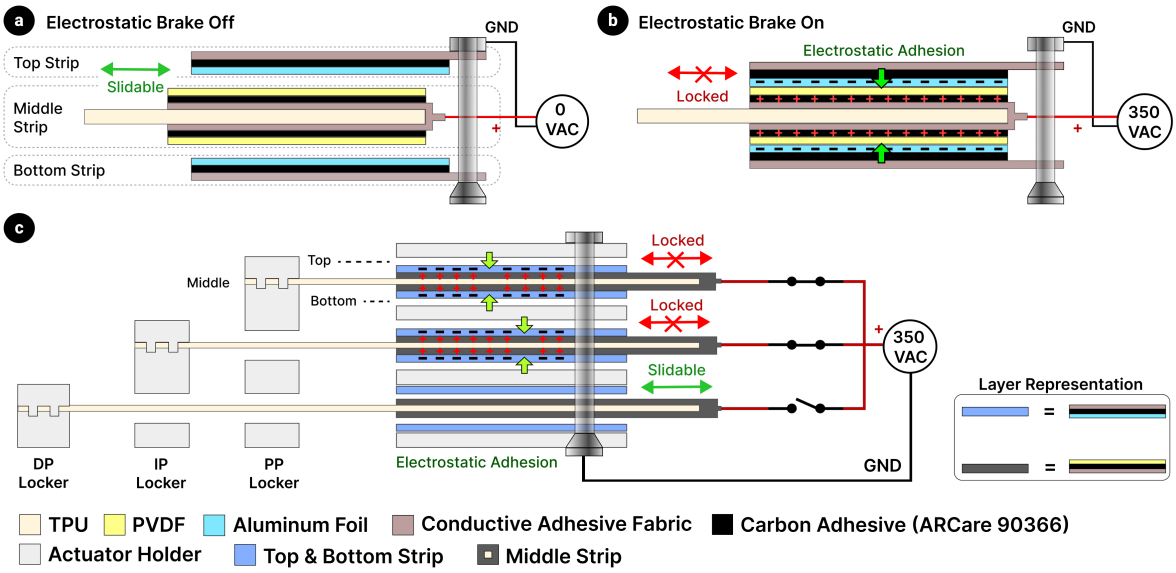

Fig. 2. Operating principle of ES clutch used in EStatiG. (a) Top and bottom strips freely slide over the middle strip when there is no difference of electrical potential (0 V). (b) When the high voltage (>200 V) is applied, electrostatic adhesion occurs to lock between layers. (c) We built EStatiG with multiple ES brakes to provide force feedback to each phalanx.

As shown in Figure 2, we form a brake that provides passive force feedback by engaging or disengaging the clutch module via electrostatic adhesion. To engage, we simply apply voltage to create jamming between layers to resist the motion of the sliding mechanism (Figure 2b). On the contrary, we apply 0 V for disengaging layers to slide over each other freely (Figure 2a). Recent haptic gloves [30, 31] have adopted the same approach, but they focused on rendering force feedback on a single phalanx of a finger which is not sufficient for full object perception upon grasp. Also, these works utilized a single side of electrodes to create braking force, which would require a large area to install the braking module.

In this work, we propose a double-layer structure for our ES clutch to maximize the overlap area, leading to higher force per unit area efficiency. Our module consists of 3 flexible strips that do not interfere with finger movement. The top and bottom strips work as conductive layers. They are electrically connected and fixed on the back of the hand. The middle strip consists of conductive materials on top and bottom and a thin dielectric layer coated on top of both surfaces. The middle strip from each module is connected to the designated phalanx to transfer the force when braking occurs. The top and bottom strips face toward the dielectric layer of the middle strip and create the electric charges on the surface by imposing the voltage through electrodes. Once enough charges are accumulated, electrostatic adhesion occurs and locks the sliding movement of the middle strip connected to each phalanx. Eventually, the movement of the finger is blocked by the braking force exerted upon activation. On the other hand, the phalanx freely slides upon deactivation when applying 0 V.

The theoretical background of the braking mechanism is described below.

$$F_{friction} = \mu F_{attraction} \tag{1}$$

$$F_{attraction} = \frac{\varepsilon_0 \varepsilon_r A V^2}{2d^2} \tag{2}$$

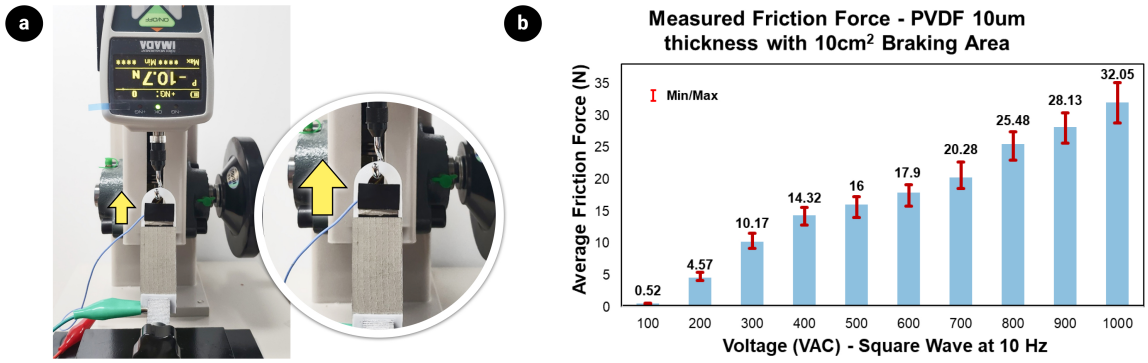

Fig. 3. Friction force measured for applied voltage between 100 V and 1000 V. The initial overlap area was 10cm^2 and the pulling speed was around 0.5 mm/s.

Equation 1 shows the calculation of a total friction force ($F_{friction}$), and μ denotes the friction coefficient. Equation 2 is derived from Coulomb's law where ε_0 is the permittivity of vacuum, which has a value of about $8.854 \times 10^{-12}\ F/m$, ε_r refers the relative permittivity (dielectric constant) of the dielectric film between the electrode, A denotes the overlap area between middle strip and other strips, d is the distance between a middle strip to either top or bottom strip (dielectric film thickness), and V is the potential difference between top-middle and bottom-middle strips. Friction force ($F_{attraction}$) refers to the force that blocks the movement of each phalanx.

We fabricated our ES clutch module with PVDF film (β-phase uniaxial orientation, PolyK) with a dielectric constant of 12 and an overlap area of 10 cm^2. Due to the presence of space charges [18, 50] that accumulate over time with the dielectric region and lower the attraction force, AC is preferred over DC as the switching of polarity can prevent the accumulation of space charges.

$$P = \frac{E}{t} = \frac{fCV^2}{2} = \frac{f\varepsilon_0\varepsilon_r AV^2}{2d} \tag{3}$$

Equation 3 shows the power required (P) to operate the ES brake where E is the energy to charge the clutch per time (t), f is the frequency, C is a variable capacitor formed by our layer structure, and V is the applied voltage between strips. To minimize the space charge and power consumption, we choose the switching frequency to be 10 Hz since the lower frequency is not fast enough to mitigate space charge. From equation 3, the required power and current can be calculated under 350 VAC with 10 Hz bipolar square wave, and the dielectric film's properties are k = 12, d = 10 μm, and area = 10 cm^2. The power consumption for each brake activation is 6.507 mW. While the single LRA has voltage and current consumption of 0.3 VAC and 12.4 mA, respectively.

The relationship between braking force at different voltage levels under the overlap area of 10 cm^2 with a dielectric thickness of 10 μm is shown in Figure 3. When ES clutch is inactivated, the free sliding friction force is maintained to be less than 0.5 N. We observed clear adhesion force appears at 200 V and increased proportionally to the increased voltage. Even though our system deploys high voltage, there is no direct contact between the user and the electricity. Moreover, our operating voltage (350 V) falls within the safe range of 300 V to 500 V, where the risk of dielectric breakdown of human skin is minimal [26]. As the current is the primary factor in electrical hazards, our system limits the current to less than 100 µA. This value is well within the safe range for human interaction, which is less than 1 mA [38].

4 SYSTEM OVERVIEW

Building a robust electrostatic haptic glove system presents several challenges. First, the material choice for creating actuation is critical, as its properties directly affect the quantity of force feedback. Here, we focused on selecting the material to ensure a balance between the quantity of generated force, durability, and release time (upon deactivation). Then, we maintained wearability by minimizing glove weight and designing mounting structures to avoid finger motion interference. Lastly, we developed a self-contained system containing a high-voltage power supply from the battery as well as a high-voltage power controller to handle up to eight ES brakes.

4.1 Fabrication of Multi-Phalanx ES Brake

Dielectric Material Selection The dielectric material is a core element that determines the performance of the ES brake. The dielectric constant and the thickness of the dielectric material are directly proportional to the electroadhesion force amplitude and required power consumption as shown in Equation 2 & 3. However, we cannot just rely on a thin dielectric layer due to durability and safety concerns. In terms of durability, the dielectric layer would be worn out with frequent activation of the ES brake and lead to short circuit damage. For safety, selected dielectric material should withstand the breakdown upon imposed voltage.

Early ES clutch work [17] used high dielectric material like a fluoropolymer embedded with barium titanate (Luxprint, Dupont) for ES clutches. Due to its brittle characteristics, however, Luxprint is not appropriate for the prototype requiring high flexibility. Although other work suggested using Kapton and PET tape [30] with ductility and high mechanical strength, dielectric constants are relatively low. To this end, researchers started to employ vinylidene fluoride-based polymers such as PVDF-HFP (k=10, E=1500 MPa) [72], and P(VDF-TrFE-CTFE) (k=40∼50, E=150 MPa) since they showed high flexibility and a relatively high dielectric constant. Recent works used P(VDF-TrFE-CTFE) as it showed the highest dielectric constant with the lowest Young's modulus [29]. However, the softness of P(VDF-TrFE-CTFE) led to stickiness and a prolonged release time after deactivation. While PVDF (k=12, E=>2000 MPa) has not been reported for use as ES clutch, the recent research [41] suggests that PVDF has appropriate electrostatic properties for ES clutch including high energy storage density, voltage breakdown, and Young's modulus. To select the appropriate dielectric material, with the similar setup in Figure 3, we fabricated the ES clutches from PVDF and P(VDF-TrFE-CTFE). Then, their release times were determined by loading both clutches with a 10 N force for 1 min and removing the load to 0 N before deactivating them. For the PVDF-based ES clutch, the release time came out as 55 ms. On the other hand, the P(VDF-TrFE-CTFE)-based ES clutch remained attached and required external force to separate them. Therefore, in this work, we selected PVDF as our dielectric material, which exhibits the balanced properties between mechanical strength and dielectric constant to support high force density while minimizing the release time.

ES Brake Structure The proposed ES clutch for activating a single phalanx consists of top & bottom strips with aluminum electrodes and one sliding strip in the middle. Figure 4 illustrates the ES brake components. For

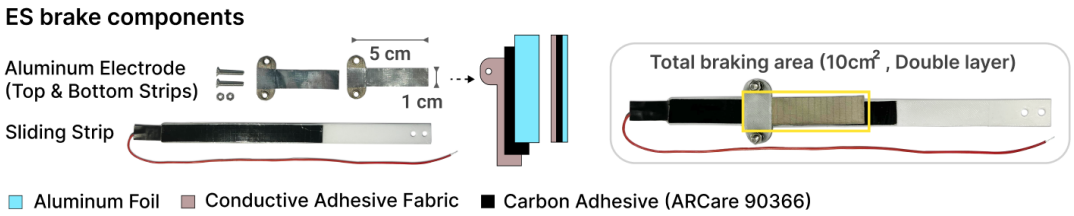

Fig. 4. A single ES brake includes two aluminum electrode strips and a sliding strip to form an overlap area of 10 cm^2.

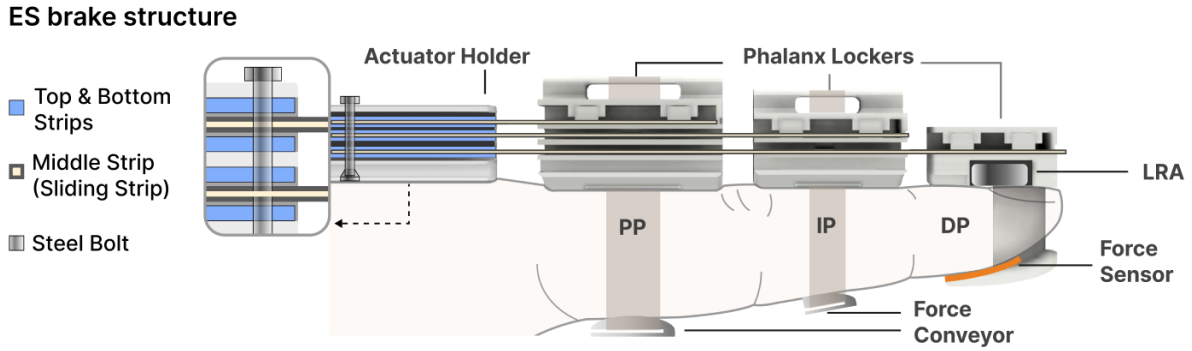

Fig. 5. The cross-section ES brake structure and components. The ES brakes are connected to all phalanges with the 3D-printed phalanx lockers.

top & bottom strips, we layered 100 μm thick conductive fabric (ID-NRA01, DImaterials) with 15 μm aluminum foil using 33 μm thick double-sided carbon adhesive (ARCare 90366, Adhesive Research). With this adhesive layer, we reduced the surface roughness and filled holes of the woven structure within the conductive fabric to increase the capacitance as suggested in [29]. Then, we laser-cut a T-shape pattern to fit into the actuator holder. We made these strips with the size of 5 cm length and 1 cm width, which formed an overlap area of 10 cm^2 when configured as a double layer. Our overall ES brake comprises 8 ES clutch connected to phalanges (3 phalanges for index and middle fingers and 2 phalanges for thumb). We made holes in the T-shape pattern to secure the top & bottom strips while maintaining electrical connections through the steel bolt.

For the middle strip (sliding strip), we used 400 μm thermoplastic polyurethane (TPU) with a width of 1.4 cm. The strip's length is covered from the actuator holder to the designated phalanx, which maintains a consistent overlap area regardless of the bending of the phalanges. We made two holes at the end of this strip to assemble with the phalanx locker. On top of the TPU base, we attached 110 μm thick double-sided adhesive tape (468MP, 3M) and laser-cut conductive fabric with a width of 1.2 cm. We left a 0.1 cm gap from the edge to prevent an unexpected short circuit. Then, we placed the 10 μm thick PVDF film using carbon adhesive with a width of 1.4 cm to cover the conductive fabric fully. We carefully processed this fabrication to prevent any wrinkles or air bubbles that deteriorate the performance and lifetime. Lastly, we connected wires at the tip of each strip and wrapped them with insulation tape.

Proof-of-concept Haptic Glove As illustrated in Figure 6, our proof-of-concept haptic glove consists of 3 actuator holders. We put these holders onto the glove using Velcro. We also attached the Velcro wrist strap to the actuator holder to fix the glove on the hand. We configured the ES brake by stacking ES clutches in the order of DP, IP, and PP (Figure 5) to transfer blocking force to each phalanx individually. We 3D printed the phalanx lockers using polylactic acid (PLA), which connects to the sliding strip. Here, we formed clutch passages inside the PP and IP phalanx lockers to allow sliding DP and IP strips. These passages also prevent potential buckling of the strips during finger bending. For IP and PP, we wrapped phalanx lockers with fabric straps clipped with a TPU force conveyor. Since the fabric can be stretchable, the force might not be well transferred to the phalange. Thus, we use the TPU force conveyor to add rigidity around the contact point to maintain the force perception. In terms of DP, the phalanx locker covers the whole fingertip to transfer the tactile sensation with added linear resonant actuators (VG1040003D, Vybronics). We mainly focused on supporting the thumb, index, and middle fingers as increasing the number of fingers does not improve the perception of the virtual objects' shape [34, 61].

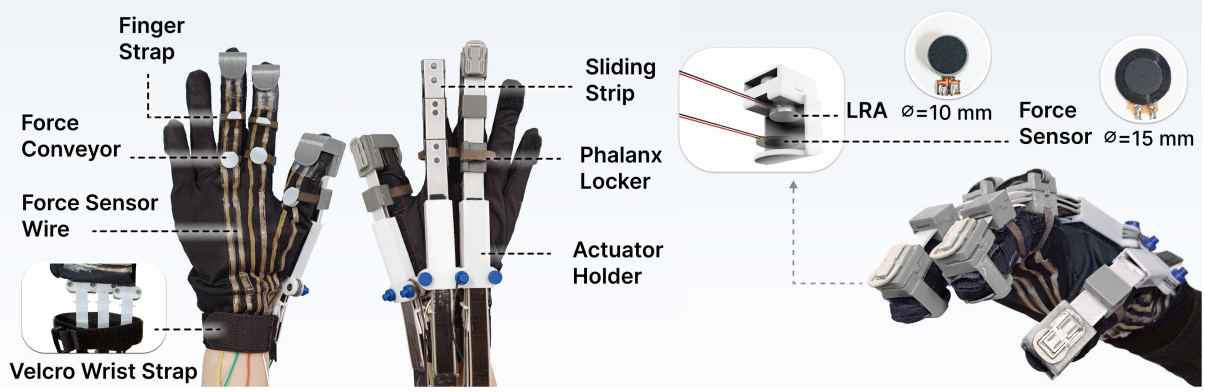

Fig. 6. Overview of EStatiG prototype and components.

We added the force sensor (RA18-DIY, Maveldex) to the fingertip to prevent engaging braking force over the system limit. We intended to measure the force applied to the fingertip when the ES brake activates. In this way, the system can detect the instance when a user is releasing the object or applying grasping force that could exceed the maximum braking force (>10N). We wired force sensors with laser-cut stretchable conductive fabric (Technik-tex P130, Shieldex) using heat adhesive (Bemis) as shown in Figure 6.

4.2 Hardware Implementation

We designed a customized control circuit as shown in Figure 7. We used a Teensy 4.0 microcontroller (600MHz ARM Cortex-M7) and connected digital pins to high voltage reed relays (131-1-A-3/1D, Pickering Electronics) to regulate the ES brakes' on/off state. Then, we employed a multiplexer (TCA9548A, Texas Instruments) with a motor driver (DA7280, Renesas Electronics) to actuate multiple LRAs. The overall dimension of the control circuit came out as 45 cm × 50 cm, which is small enough to be mounted on the arm. To make a battery-powered portable high voltage supply (>200 V), we referred and modified [49] to further create bipolar square wave signals from 6 VDC. Here, we added two additional optocouplers and MOSFETs to form an H-bridge and drove the extra MOSFET with the inverse signal from the output of the original MOSFET. The total weight of our gloves comes out as 180 grams (130 grams for the gloves and 50 grams for the control circuit). The ES brake weighs only 10 grams per phalanx.

5 TECHNICAL EVALUATION

We carried out technical evaluations to confirm the performance of our ES brake. Here, we explored the durability by testing the activation cycle and force feedback capability by measuring the force transferred to each phalanx.

5.1 Fatigue Life

For this evaluation, we repeatedly activated the ES brake and applied the load until the electrodes slipped from each other when reached the maximum braking force. In this manner, we measured the realistic fatigue life of the proposed ES brake. We used the same setup to measure the friction force (Figure 3), where we connected the sliding strip to the push-pull gauge (ZTA-200N, Imada) while another electrode was fixed to its base.

For testing, we used a 10 μm thick PVDF with an operating voltage of 350 VAC at 10 Hz and an overlapped area of 10 cm^2, identical to the implementation conditions. This setup supports an average braking force of 12.28 N. During 500 trials, we observed a force range of 10.8 N~13.7 N, with no significant decrease in braking force.

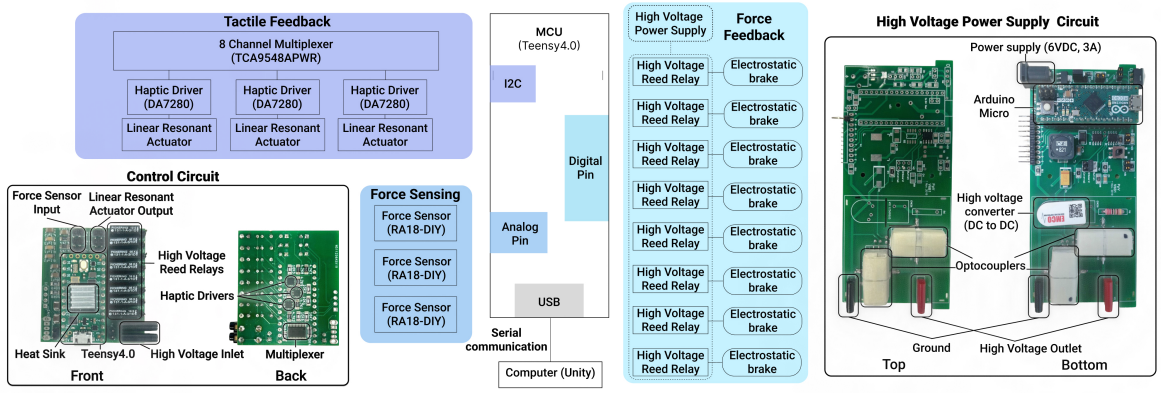

Fig. 7. Multi-phalanx ES brake circuit diagram. We employed ES brakes and LRAs to create force and tactile sensation. Our control circuit and portable high-voltage supply enabled force feedback sensation on multiple phalanges.

5.2 Force Feedback Validation

Since our ultimate goal is to provide braking force to each phalanx for grasp, it is critical to assess how much force is actually transferred to each phalanx with our prototype. To measure the reaction force acting on the phalanx, we installed the calibrated force sensor (RA18-DIY) for testing purposes. We also added two force sensors to the Velcro wrist strap to measure the anchoring force, which is the force exerted to fix the wrist strap from moving during grasping. This force was determined by how much we wrap the strap around the wrist. We then examined the relationship between the maximum anchoring force and the transferred force. For the evaluation, we activated the braking force of 12 N for each phalanx and instructed users to perform full grasp, to obtain the maximum transferred forces. A total of 12 participants were recruited (6 women and 6 men; Mean=27 years old, SD = 3.8). Each of them performed 72 trials (8 locations × 3 anchoring forces × 3 set). Throughout the experiment,

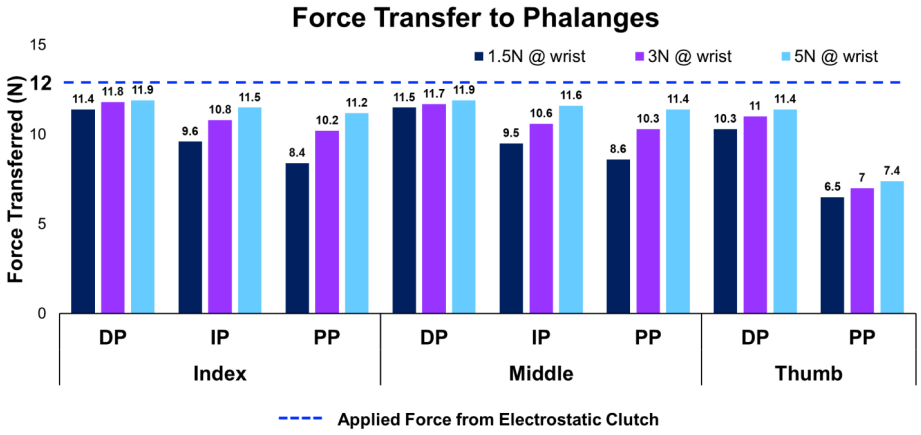

Fig. 8. The ES brake transferred force to each phalanx for 3 different wrist anchoring forces (1.5 N, 3 N, and 5 N). ES brake provided a maximum of 12 N (350 VAC with 10 Hz and an overlap area of 10 cm^2.)

the brake occasionally slipped when the measured force exceeded 11 N. When this happened, we recorded the last measured force before the slip as the maximum transferred force.

Figure 8 illustrates the results of our evaluation. On average, we observed the force transfer rates of 95%, 80%, and 70% on DP, IP, and PP for index and middle fingers when anchored on the wrist with 1.5 N. With the increase in wrist anchoring force from 1.5 N to 5 N, we saw a high increase in force transfer rates (more than 90% on average). The DP exhibited a high force transfer rate because the phalanx locker covers the whole fingertip with the rigid body. On the other side, IP and PP showed less force transfer since the force was transferred through flexible TPU conveyors. For the thumb, PP has a significantly lower force transfer rate. We assume this is due to the anchoring point of the thumb's PP being located around the Carpometacarpal joint (CMC), which naturally moves along the motion of the thumb's PP. Apart from the force transfer efficiency validation, we also evaluated how multi-phalanx improved the angle position perception performance in User Study 1.

6 HAPTIC RENDERING WITH ESTATIG

Previously, the force feedback on phalanges has been suggested [3]. However, users' capability to distinguish the applied forces at different phalanges and how users perceive the blocking forces at multiple phalanges have not been fully explored. To address this gap, we carried out an exploratory study to find out two key aspects of human force perception on the finger: (1) the accuracy of force localization across different phalanges and (2) the perceived force patterns when blocking forces presented at multiple phalanges. We utilized the findings from the study to form ES brake actuation conditions to provide effective and efficient force feedback.

6.1 Exploratory Study

Our exploratory study had two main sessions. In the first session, users identified the perceived location of the braking force during the grasp. Our prototype activated an ES brake on a single phalanx location. The possible phalanx locations included the Distal Phalanx (DP), Intermediate Phalanx (IP), and Proximal Phalanx (PP) of

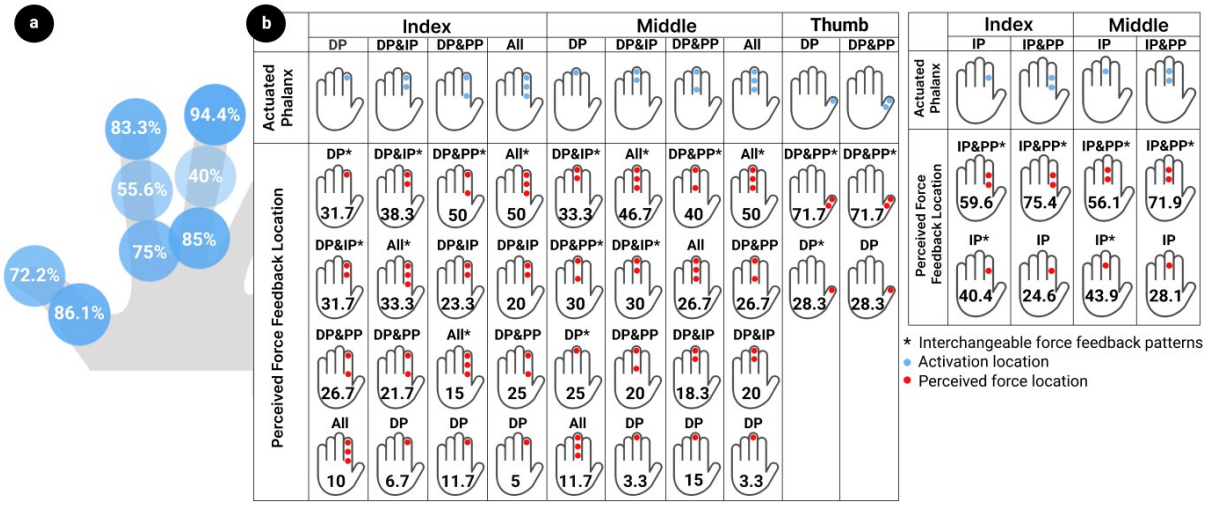

Fig. 9. The result of an exploratory study on force localization perception accuracy with EStatiG. (a) Identification accuracy when a single braking point was applied at a single phalanx, (b) Perceived force feedback location distribution (in percentage) when multiple braking points were applied at multiple phalanges.

the index, middle, and thumb, as shown in Figure 9a. Then, participants identified the perceived location of the phalanx. Users carried out a total of 24 trials (8 locations × 3 set).

In the second session, we conducted a study to investigate how users perceived the force across the finger segments for different combinations of multi-phalanx force feedback. We had a total of 14 different combinations of multi-phalanx force feedback patterns shown in Figure 9b. We configured DP dominant tasks and IP dominant tasks where we supported constant braking force to DP or IP while activating braking force in various patterns. Moreover, we had cases with braking force activated on all phalanges for each finger. Participants carried out a total of 42 trials (14 patterns × 3 set). The entire study lasted about 40 minutes.

We recruited 16 participants (9 women and 7 men; Mean=26 years old, SD=4.1) and asked them to wear our haptic glove on their dominant hand. They were fully instructed about our user study and consented before the study. We operated the device at 350 VAC at 10 Hz, creating a maximum of 12 N braking force. Before conducting the test, we activated all phalanges individually to familiarize participants with the sensation of force from our device. During the study, we blindfolded participants to remove the bias caused by the visual information from the sliding strip movement. Then, we asked participants to bend their hands slowly and verbally answer which phalanx was being blocked.

Results and Discussions In the first session, the participants showed an overall perception accuracy of 74% in detecting the location of the phalanx with applied braking force (Figure 9a). We observed that the DP of the index and middle showed the highest accuracy within a finger, as expected, with DP's high sensitivity [36]. The braking force at IP had the lowest accuracy in the index and middle because participants often misinterpreted sensation on IP as that on PP. We assume this was due to the hierarchical finger bone structure, where we observed that blocking IP made PP hard to move as well.

The effect of hierarchical bone structure of also showed in the second session, as our investigation found that common confusions occurs when providing braking force for the adjacent phalanx. For examples, by only providing a force on DP created a sensation on DP as well as DP&IP, and giving forces DP&IP could felt like all phalanges were blocked. In the case of thumb, 71.7% of participants reported the sensation of the force feedback on

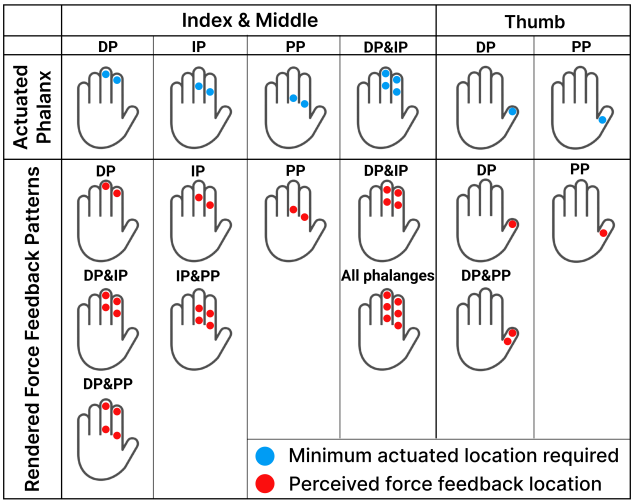

Fig. 10. Designated haptic rendering patterns for applying ES brake(s) (blue dots) to stimulate various force feedback patterns (red dots).

DP&PP regardless of applied braking force patterns. From these results, we drew interchangeable force feedback patterns as illustrated in Figure 9b. Our study unveiled that we could activate fewer ES brakes to elicit a similar sensation compared to activating whole intended phalanges.

6.2 Haptic Rendering Algorithm

To formulate power-efficient rendering while maintaining performance, we employed a study-informed approach for haptic rendering. Rather than activating every phalanx in contact with a virtual object, we leveraged insights from the exploratory study. If the perceived percentage of certain patterns was higher or within a 5% difference compared to the perceived percentage of the actual actuated phalanges, could indicate that actuating only those specific phalanges was sufficient to render the desired force feedback sensation. As a result, we identified a minimal set of ES brakes to activate while maintaining similar perceived force patterns for the user (Figure 10). The blue dots in Figure 10 represent the efficient rendering pattern, which can effectively render the red dot patterns in the same column. Here is an example of how we utilized perceived force patterns to render power grasp where the PP collides with the object first, followed by the IP, and the DP. Initially, the ES brake of the PP is activated (as the PP represents only itself). When the IP makes contact with the object, the ES brake of the PP is deactivated, and the ES brake of the IP is activated (with the IP representing IP&PP). Finally, once the DP contacts the object that completes the grasp, the ES brake of the DP is activated (with the DP&IP representing all phalanges). A similar mechanism is observed in the thumb. The ES brake of the thumb's PP is activated upon its collision with the object and is subsequently deactivated when the thumb's DP contacts the object. At this point, the ES brake of the thumb's DP is activated, with the DP representing the DP&PP for the thumb. We then further evaluated the effectiveness of our adaptive rendering algorithm in the User Study 2.

Figure 11 illustrates our overall haptic rendering pipeline. We rendered the haptic feedback based on the collision detection between the virtual objects and the phalanges during the grasping interactions. We obtained hand-tracking data from the motion capture gloves module (Quantum Gloves, Manus Meta), which was mounted

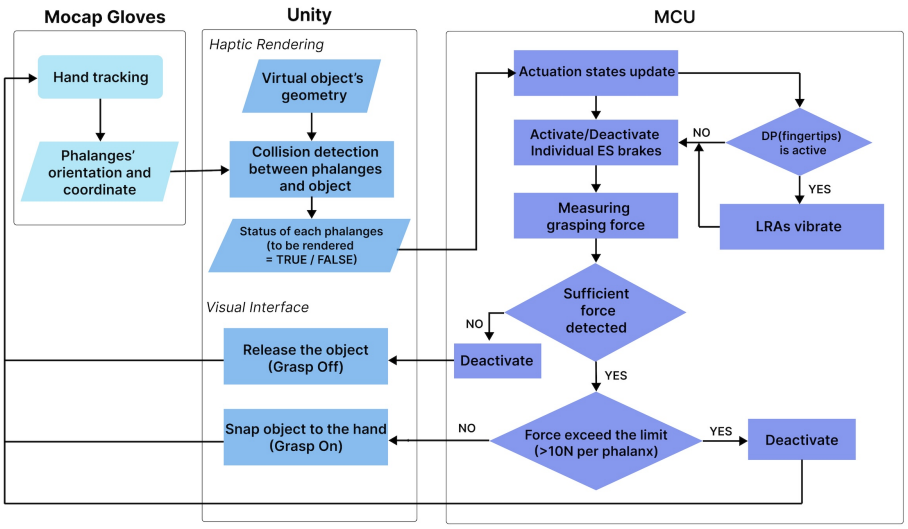

Fig. 11. Haptic rendering pipeline of EStatiG. We employed haptic rendering patterns from the exploratory study to support force feedback on multiple phalanges for the index, middle, and thumb.

on top of our prototype. Whenever the virtual phalanges were in contact or out of contact, the changes in the status of that phalanx were sent to the MCU. Based on the haptic rendering patterns set in Figure 11, our system determined activation of ES brakes accordingly (Actuation states update in Figure 11).

For the tactile feedback, the LRAs vibrated when the DP state changed from inactive to active state to simulate the sensation of touching the objects' surface. Using the force sensor attached to each fingertip, we could check the physical status of the applied force to the user. Based on the force measurement, the virtual object was either snapped or released from the hand. We also monitored the force measurement to prevent damaging the ES brake by disengaging the brake when the applied force almost reached the maximum braking force (>10 N).

7 USER STUDY

In the user study, we investigated both the objective and subjective performance of EStatiG compared to the conventional single-phalanx force feedback approach. For the objective assessment, we evaluated users' accuracy in identifying different finger phalanx-angle positions. In the subjective study, we explored users' experiences during interaction with primitive object shapes using our approach versus the baseline. Through these studies, we verified the effectiveness of the proposed multi-phalanx ES brake for shape perception and gained valuable insights into the user experience with our approach.

7.1 User Study 1: Phalanx-Angle Position Perception

In User Study 1, we carried out a within-subject study to determine the perceivable angle resolution. We quantitatively measured the performance of multi-phalanx force feedback by validating how many levels of bending could be perceived. The tasks required participants to bend their hands around different joints, which mimicked grasping objects with various shapes and angles. In addition, we compared our multi-phalanx approach with the single-phalanx method and hypothesized that the multi-phalanx force feedback approach would enhance the user's ability to perceive and distinguish various angles of finger bending more accurately. We believed multi-phalanx force feedback has the potential to offer more detailed information about the position and movement of the fingers. An increased number of sensory inputs might improve the user's ability to discern different angles.

Study Setup We recruited 17 participants (7 women and 10 men; Mean=26 years old, SD=4.43). All participants were right-handed and did not have a problem with wearing the prototype. The overall study took about 2 hours.

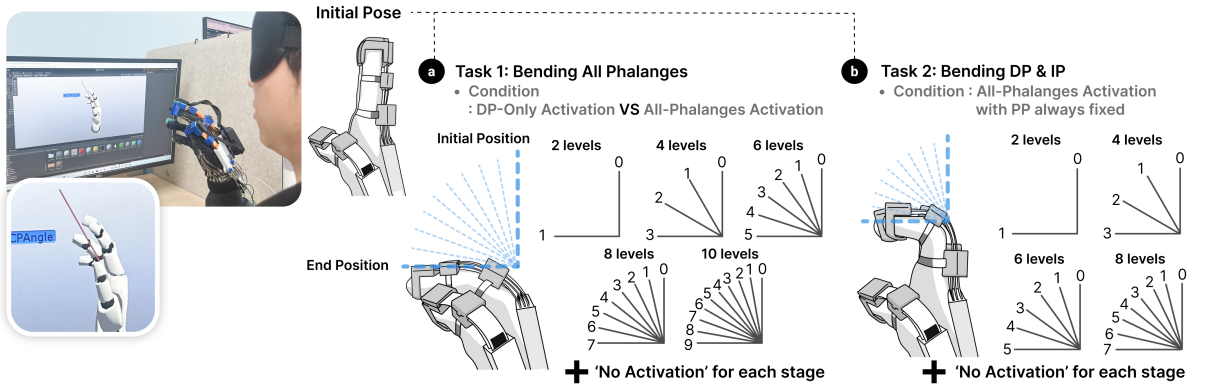

Fig. 12. Finger phalanx-angle positions perception test study setup. (a) Bending all phalanges together for 5 different stages (including 2, 4, 6, 8, and 10 levels) and (b) bending DP&IP together, while PP was fixed for 4 different stages (including 2, 4, 6, and 8 levels). Both (a) and (b) contained 'No activation' condition for each stage.

We equipped participants with a headphone playing white noise and blindfolds to prevent bias from auditory or visual cues.

In this study, participants carried out two tasks including all-phalanges bending task (Task 1) and DP&IP phalanges bending task (Task 2) as shown in Figure 12. For Task 1, we asked participants to bend the whole phalanges of the index and middle finger around the metacarpophalangeal (MCP) joints. For Task 2, we instructed participants to bend their DP and IP phalanges around the proximal interphalangeal (PIP) joints while the PP were fixed by keeping them activated. The wrist position was fixed as a pivot point in the virtual scene. Our system activated the ES brake to provide force feedback when the position of the phalanges reached a certain degree of angle, which was randomized and counterbalanced for the trials.

Task 1 consisted of five stages with different angular resolutions. We divided 90 degrees into 2, 4, 6, 8, and 10 levels for each stage, and the degrees between each level were 90°, 30°, 18°, 11.3°, and 10°, respectively. Task 2 covered four stages where we divided 90 degrees into 2, 4, 6, and 8 levels. We also included the 'No Activation' case in every stage for both tasks where no force feedback was provided to fingers. Therefore, the number of answer options in each stage were 3, 5, 7, 9, and 11 in Task 1 and 3, 5, 7, and 9 in Task 2 accordingly. We did not conduct a study on DP bending with the fixation of IP and PP because the flexion and extension movement range was limited below 40° [58] which was insufficient to provide meaningful angle divisions for the force feedback.

For Task 1, we provided two activation conditions including DP-only (DPA) and all-phalanges activations (APA) and compared the results. In Task 2, we only conducted all-phalanges activation conditions. All stages were repeated twice except the first stage discriminating 2 levels, where we repeated 3 times to get a sufficient number of data. Figure 12 illustrates the overall design of our User Study 1.

Study Procedure We ran a walkthrough session where participants went through all conditions to get acquainted with the system and reference cues. Participants verbally responded at which level they felt the blocking force. If they didn't feel any resisting force, they answered it as 'No Activation'. After repeating the same stage twice (3 times for the first stage), we moved on to the next stage. Between Task 1 and 2, we offered a 10-minute break. We carried out a total of 197 trials (73 trials for Task 1 with stage repetitions × 2 activation conditions, 51 trials for Task 2 with stage repetitions) and collected 3349 (197 trials × 17 participants) responses.

Results In Task 1, we averaged accuracy rates across all levels within each stage, thereby obtaining the accuracy rate for each stage. Furthermore, we compared the accuracy rate of the same stages between two

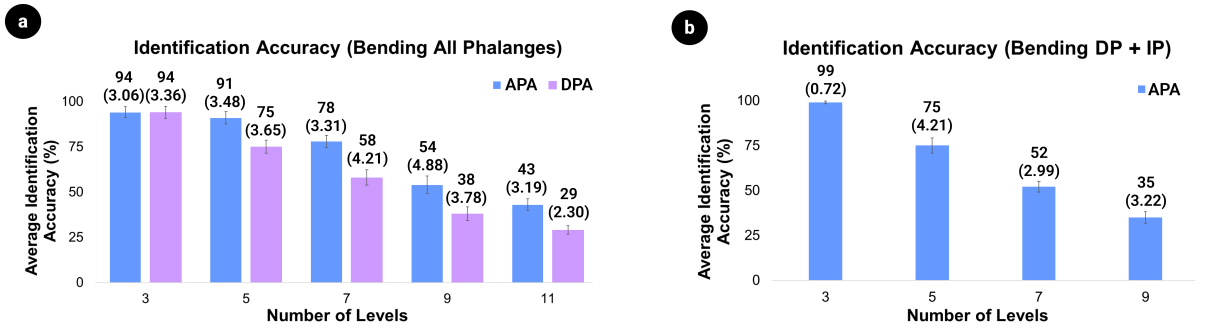

Fig. 13. The average identification accuracy of the phalanx-angle positions perception test. (a) The comparison of identification accuracy between all-phalanges activation (APA) and DP-only activation (DPA) conditions when all phalanges were bending together and (b) the identification accuracy of all-phalanges activation condition when bending DP and IP while PP was fixed. The error bars represent standard errors.

activation conditions: DPA and APA, as shown in Figure 13a. For more details on the result, please refer to **Appendix B**.

Overall, results showed that DPA had a steeper decline in accuracy as the number of levels increased. On the contrary, APA maintained a relatively high accuracy where it showed >90% accuracy for identifying 5 different levels of bending angles. Still, we observed a significant drop in both conditions when the number of levels increased to 7 or above. Therefore, we confirmed that our device can support clear sensation of angle resolution of 18° for most users and showed superior performance compared to DPA. For Task 2, we found out that our device can support rendering the angle resolution of 30° when bending around the PIP joint, which was lower than bending around the MCP joint.

In this study, we confirmed that our approach of utilizing all phalanges for force feedback superseded existing DP-only force feedback. As we expected, stabilizing the position of a finger appropriately using the APA condition contributed toward better performance.

7.2 User Study 2: Object Perception Experience

In Study 2, we evaluated the overall experience of using EStatiG while grasping virtual objects with primitive shapes. We compared the subjective ratings of three ES brake activation strategies, including DP-only (baseline), all-phalanges, and all-phalanges with our haptic rendering pipeline from Figure 11. According to User Study 1, the all-phalanges activation condition could help users perceive high-resolution angles compared to the DP-only activation condition. In addition, during the exploratory study, we discovered that our haptic rendering algorithm could cover the sensation of all-phalanges activation while activating fewer phalanges. Therefore, we hypothesized that all-phalanges adaptive activation with our rendering approach (ADA) and all-phalanges activation (APA) conditions would provide a better user experience than DP-only activation (DPA) condition, while ADA has no significant difference from APA. We also obtained qualitative user feedback to address the limitations for future development.

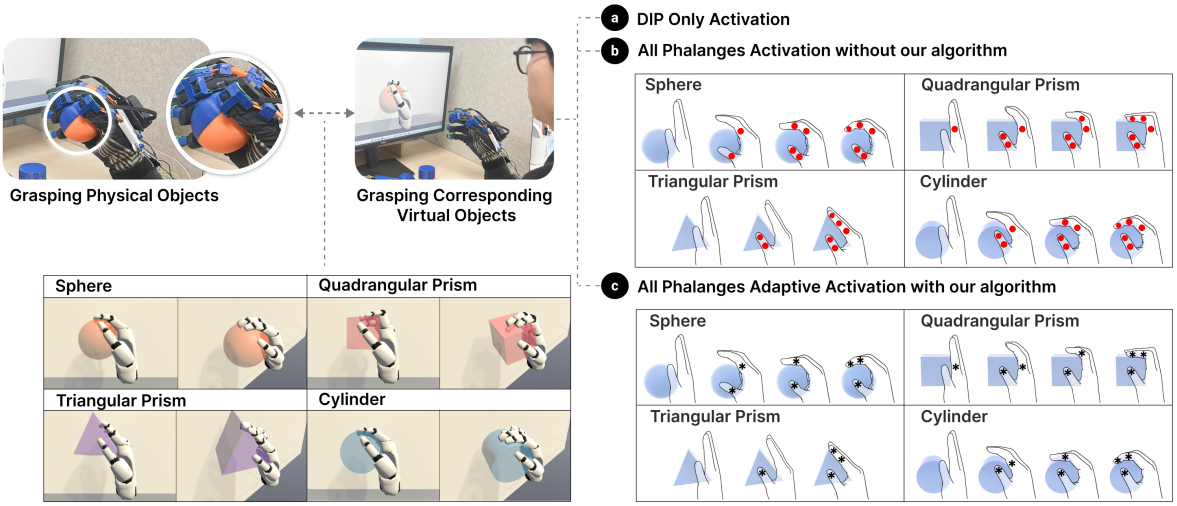

Fig. 14. Object perception study with sphere, quadrangular prism, triangular prism, and cylinder using 3 haptic feedback conditions including (a) DP-only activation (DPA), (b) all-phalanges activation (APA), and (c) all-phalanges adaptive activation (ADA, our haptic rendering method).

Study Setup We carried out a within-subject design experiment where all participants explored identical objects for 3 different conditions. The participants were the same group from User Study 1, except for one participant who withdrew due to personal reasons. The overall study took about 30 minutes. In this study, we guided participants to watch the monitor displaying VR scenes where their virtual hands interacted with virtual objects. We also offered 3D-printed physical objects that had the same geometry as testing virtual objects, so users could refer to these objects as the ground truth.

We provided 4 objects with various shapes such as sphere, quadrangular prism, triangular prism, and cylinder. For this test, we fixed the virtual hand position and let users only perform grasping actions. This allowed participants to focus solely on the grasping motion. Figure 14 illustrates the overall sequence of Study 2.

We asked participants to provide subjective ratings for all conditions by answering 5 questions related to 5 haptic experience keywords [21, 57] (Realism: *How realistic was the feeling of the object?* , Comfort: *How comfortable was the interaction?* , Immersion: *How does haptic feedback increase your involvement in grasping?* , Harmony: *How appropriate is the haptic feedback on where and when you felt it?* , and Satisfaction: *How do you like having haptic feedback as part of your experience?*). Participants rated using a 7-point Likert scale ranging from 1 to 7 through the online form via tablet.

Study Procedure After participants received ground truth sensation of physical objects, we asked participants to grasp the virtual object. We presented virtual objects in randomized order. For the presented object, all activation conditions were given in a random order without disclosing condition information. We guided participants to thoroughly explore each condition's sensation until they felt confident enough to respond to the questionnaire. We collected a total of 960 data points (4 objects × 3 haptic rendering conditions × 5 questions × 16 participants). After the study, we had a brief interview session asking about the overall experience of interacting with virtual objects with given force feedback conditions.

Results To assess the impact of haptic activation conditions on each keyword across different objects, we employed the Wilcoxon signed-rank test for analysis, as depicted in Figure 15. Since we did not observe a significant difference between ADA and APA conditions, we only compared it with the DPA condition. We

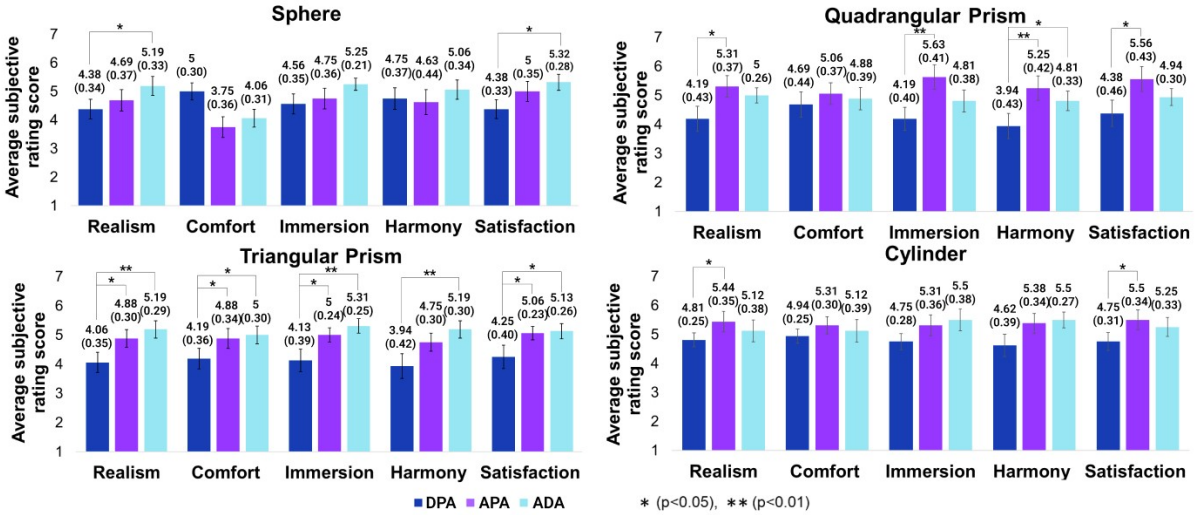

Fig. 15. The object perception experience ratings for various haptic feedback conditions. Each bar graph refers to the subjective rating from the participant under five criteria including realism, comfort, immersion, harmony, and satisfaction.

observed a significant enhancement in the overall experiences with the quadrangular and triangular prism but a relatively small enhancement in realism and satisfaction with the sphere and cylinder.

Significant differences were observed across various keywords. (i) For realism, distinctions were found between DPA and APA conditions for the quadrangular prism (p = .026 < 0.05), triangular prism (p = .031 < 0.05), and cylinder (p = .04 < 0.05), as well as between DPA and ADA conditions for the sphere (p = .021 < 0.05) and triangular prism (p = .003 < 0.005). (ii) Comfort ratings displayed significant differences, particularly with the triangular prism, between the DPA and both APA (p = .04 < 0.05) and ADA conditions (p = .026 < 0.05). We also found that the subjective rating of comfort for the sphere with APA and ADA conditions was lower than with the DPA condition. (iii) Immersion showed statistically significant distinctions between the DPA and APA conditions for the quadrangular (p = .003 < 0.005) and triangular prism (p = .026 < 0.05), and between DPA and ADA conditions for the triangular prism (p = .007 < 0.05). (iv) Harmony ratings exhibited significant differences between the DPA and APA conditions with the quadrangular prism (p = .005 < 0.05), and between DPA and ADA conditions for both quadrangular (p = .021 < 0.05) and triangular prisms (p = .005 < 0.05). (v) Lastly, satisfaction ratings differed significantly between the DPA and APA conditions across all objects, including the sphere (p = .022 < 0.05), quadrangular prism (p = .01 < 0.05), triangular prism (p = .032 < 0.05), and cylinder (p = .031 < 0.05), with additional notable differences between the DPA condition and ADA condition for the triangular prism (p = .032 < 0.05).

Qualitative Feedback We received feedback from 5 participants that the quadrangular and triangular prisms provided the most realistic sensation of grasping. This is probably because multi-phalanx sensations were emphasized with these objects compared to rounded shapes. We also received a comment that the sensation of manipulating the thumb was weaker than that of other fingers. We assumed that different ranges of movement for the thumb were not notably different by objects. Lastly, two participants mentioned that as the wrist and object positions were fixed, they could not fully manipulate the objects, including dragging or rotating, which led them to rate low scores for immersion regardless of activation conditions.

8 APPLICATIONS

EStatiG delivers multi-phalanx haptic feedback to enhance the immersive experience of interacting with varied virtual objects. Its lightweight structure and responsive haptic feedback, along with an efficient haptic rendering algorithm, make it suitable for several applications. EStatiG can be utilized in both industrial and personal contexts. We propose use cases for our device in industrial training, remote control, entertainment, and telepresence.

Industrial Training Nowadays, industries adopt VR training to reduce the cost and relax the time-space restriction [5]. As the study suggests [24], with the presence of haptic feedback, task learnability has improved, especially for complex assembly tasks. Since EStatiG enables haptic sensation on multilateral shapes, it is suitable for VR training scenes that deal with industrial tools. By allowing users to feel like they are touching the machinery, we can closely replicate the actual industrial environment to enable effective training.

Teleoperation The current teleoperation systems utilize handheld controller devices or bare hands to control the robot which can be difficult to precisely grasp or manipulate virtual objects. EStatiG can potentially contribute to improving the performance of teleoperation. By accurately rendering the shape of the object, EstatiG allows users to perceive the richer sensation of the size, shape, and texture of the objects, leading to better control over grip strength and end effector placement. Moreover, relying less on visual cues and more on haptic sensation to understand the object and adjusting the grasp accordingly can reduce the operators' cognitive load [9].

Entertainment VR entertainment contents usually ask users to use controllers to manipulate the virtual objects. However, conventional controllers simply pass through objects without any haptic sensation, which reduces the immersion and gives a sense of artificiality. In particular, games that interact with organic shapes like bouldering, where users touch and grab rocks with multi-edge geometry, require a haptic sensation on

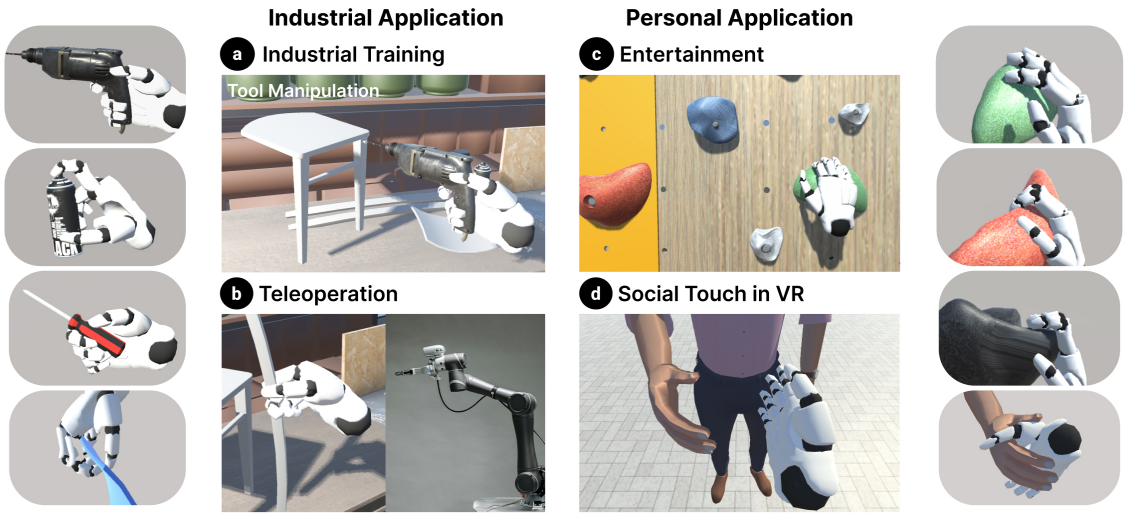

Fig. 16. Example use case scenarios showing (a),(b) industrial applications and (c),(d) personal applications.

intermediate phalanges (IP) and proximal phalanges (PP) as described in Figure 16 c. Using EStatiG, the detailed haptic feedback from the phalanges can provide greater immersion in VR scenes.

Social Touch in VR In a VR scene, socially interacting with other characters is a crucial part of the experience. Social touch is one way of nonverbal communication through physical contact. Experiencing social touch in a VR scene can increase intimacy towards the character and enhance the social telepresence [32]. For users to physically interact with the virtual characters, the device being used needs a haptic feedback functionality. As EStatiG provides both tactile and force sensations in the hand, it is applicable for interacting with characters similar to real-life situations.

9 DISCUSSION

After thoroughly examining our multi-phalanx haptic glove, we analyze the evaluation results in detail, highlighting performance improvements and issues encountered during the design and implementation process. Following that, we provide guidelines for selecting haptic rendering methods and make recommendations based on our findings to improve user experience with diverse object shapes. Finally, we propose future work directions, including hardware enhancements and additional user study scenarios, to advance the applications of our haptic glove.

9.1 Evaluation Result Analysis

Several studies have implemented multi-phalanx haptic gloves [3, 40]. Nevertheless, these approaches typically relied on conventional electric motors, resulting in bulky structures and high power consumption. To address these limitations, we adopted the ES brake for its lightweight design (10 grams per brake) and low power consumption. However, challenges arose in dielectric material selection and designing for fast engagement and disengagement. Through multiple design iterations, we achieved a balance between critical aspects including wearability (lightweight with comfort), force feedback capability (12 N braking force per phalanx), and manufacturability (low-cost & in-house fabrication process).

Our user experiments demonstrated significant improvements in phalanx-angle position perception and user experience compared to a baseline with blocking force applied only to the DP. In User Study 1, while the all-phalanges activation condition yielded better performance, the achieved angle resolution of 18° exceeded the Just Noticeable Difference (JND) of the PIP and MCP joints (1.7°∼2.7°) which are measured when the hand is in contact with physical objects [63]. The difference in angle resolution between our results and the JND could be attributed to the deformation of the soft fabric glove used as a base for component attachment for wearability, instead of rigid structures. Despite efforts to tighten the Velcro strap on the wrist to prevent displacement during finger flexion, achieving perfect fixation was unattainable and caused discomfort, leading to inevitable deviation errors from the target point. User Study 2 revealed similar overall performance between our haptic rendering pipeline (ADA, derived from the exploratory study) and the all-phalanges condition (APA, force applied to all phalanges). For quadrangular prism, a strong and rigid force using APA condition was preferred, whereas for objects with flat, tilted surfaces such as triangular prism which require similar rotation across all phalanges, ADA method was favored. The impact of multi-phalanx activation was minimal for the sphere and cylinder.

9.2 Guideline for Haptic Rendering Selection

To understand these preferences and provide guidelines for various object shapes, we further analyzed the interaction mechanism. (i) For objects that required angular representation between the PP and IP, activation of these two phalanges accurately represented the angle and maintained a firm grasping sensation. This influenced the overall preference for the APA condition over the ADA and DPA conditions. (ii) For objects with flat and inclined surfaces, no sequential activation was required. Additionally, the exploratory study indicated that the angular representation around the MCP joint by activating the PP could be substituted by activating the IP when accompanied by DP activation. As a result, APA can be replaced by only activating essential phalanges determined by ADA. (iii) For objects with curved surfaces, activation of both APA and ADA conditions may create a perception of discrete angles between the phalanges, impairing the sensation of touching the continuous curvature. This could explain the minimal difference in preference among all activation conditions. Yet, the initial touch sensation with the PP might enhance the perception of grasping the object better than the DPA condition, accounting for the slightly higher overall preference for the ADA condition compared to other activation conditions. We propose guidelines for interpreting and generalizing our results based on these findings. The APA condition is recommended to provide a better sensation of grasping for objects that need to render exact angles between phalanges. The ADA condition is more efficient for an improved user experience for objects with flat, and sloped surfaces. Lastly, for objects with curved surfaces, designers can choose either the DPA or the ADA method based on the desired sensation. If the goal is to emphasize the smoothness of the curvature, the DPA method is recommended. Conversely, if the focus is on enhancing the grasping process of the curved object, the ADA condition is more suitable.

9.3 Future Work

We acknowledged that our studies mainly looked at four basic shapes that required users to make hand poses at different angles, such as flat surfaces, right angles, and curve, by bending their fingers. To expand the scope of our interaction methods, future research should focus on more complex shapes and settings. This includes testing objects with complex geometries, such as irregular polyhedra or organic shapes, as well as objects that combine different geometric features like concave and convex areas. Future studies with complex shapes would help us better understand how well our current haptic feedback methods work with a wide range of objects and would provide deeper insights into the strengths and limitations of our approach.

In addition to examining a broader set of shapes, it is important to include more dynamic interactions in our study. We focused on isolating the grasping interaction by fixing participants' hand positions and conducting a

controlled environment study to investigate the user's ability to securely grasp objects with the device. However, realistic and immersive object interaction involves not only grasping but also object manipulation, including object translation and rotation. Future iterations should explore user performance in these more interactive and actively engaging tasks. The evaluation of the user experience during object manipulation with the device would enable us to assess how effectively the device replicates the haptic sensation users have with real-world objects in diverse contexts.

To enhance the feasibility of various grasping postures and objects, the hardware design may be revised through certain modifications. Greater freedom in abduction and adduction movements can be achieved by using a cable or tendon instead of a TPU strip to transmit the resisting force. However, additional springs might be required to prevent buckling, which can add more free sliding friction to the system. The design also requires improvement in transferring braking force to the thumb's PP through a mechanism that resists unwanted CMC joint movement. Apart from shape rendering, our haptic glove uses LRAs, but we have not experimented with actuating LRA at different durations and amplitudes. This can improve the representation of texture and stiffness of objects. [65] For hand tracking, the current system employs an external hand-tracking system. This adds 80 grams of weight and introduces potential inaccuracies since this tracking system was originally designed for bare-hand usage. As mentioned in prior works [30, 31], developing self-sensing capabilities by tracking capacitance changes in our three electrode pairs per phalanx can enable more robust hand tracking in the future.

10 CONCLUSION

In this work, we present EStatiG, a novel wearable haptic feedback system with multi-phalanx ES brakes. We aimed to enhance object shape recognition during grasping in VR. We designed and fabricated EStatiG gloves. Then, we conducted a user study to explore the feasibility of rendering force feedback on multiple phalanges for enhancing object perception compared to single-phalanx feedback at the fingertips. Our results showed that EStatiG's multi-phalanx force rendering significantly increased realism, immersion, and user satisfaction during interaction with various shapes. This effect was particularly noticeable for objects with intricate shapes, such as triangular prisms and cubes, where multi-point feedback provided a more accurate representation of the object's edges and contours. We hope our work paves the way toward more realistic and immersive VR experiences.

11 ACKNOWLEDGMENTS

This work was supported by the National Research Council of Science & Technology (NST) grant by the Korea government (MSIT) (No. CRC21011), the National Research Foundation of Korea (NRF) grant funded by the Korea government (MSIT) (No. 2022R1A4A5033689), and Electronics and Telecommunications Research Institute (ETRI) grant funded by the Korean government [24ZC1200, Research on hyper-realistic interaction technology for five senses and emotional experience].

REFERENCES

[1] Merwan Achibet, Géry Casiez, and Maud Marchai. 2016. DesktopGlove: A multi-finger force feedback interface separating degrees of freedom between hands. In *2016 IEEE Symposium on 3D User Interfaces (3DUI)*. IEEE, 3–12.

[2] Kota Amano and Akio Yamamoto. 2011. An interaction on a flat panel display using a planar 1-dof electrostatic actuator. In *Proceedings of the ACM International Conference on Interactive Tabletops and Surfaces*. 258–259.

[3] Siyeon Baik, Shinsuk Park, and Jaeyoung Park. 2020. Haptic Glove Using Tendon-Driven Soft Robotic Mechanism. *Frontiers in Bioengineering and Biotechnology* 8 (2020). https://doi.org/10.3389/fbioe.2020.541105

[4] Jonathan Blake and Hakan B. Gurocak. 2009. Haptic Glove With MR Brakes for Virtual Reality. *IEEE/ASME Transactions on Mechatronics* 14, 5 (2009), 606–615. https://doi.org/10.1109/TMECH.2008.2010934

[5] Prawit Boonmee, Benchaporn Jantarakongkul, and Prajaks Jitngernmadan. 2020. VR Training Environment for Electrical Vehicle Assembly Training in EEC. In *2020 - 5th International Conference on Information Technology (InCIT)*. 238–242. https://doi.org/10.1109/InCIT50588.2020.9310947

[6] C.W. Borst and A.P. Indugula. 2005. Realistic virtual grasping. In *IEEE Proceedings. VR 2005. Virtual Reality, 2005.* 91–98. https://doi.org/10.1109/VR.2005.1492758

[7] Christoph W Borst and Arun P Indugula. 2005. Realistic virtual grasping. In *IEEE Proceedings. VR 2005. Virtual Reality, 2005.* IEEE, 91–98.

[8] Mourad Bouzit, Grigore Burdea, George Popescu, and Rares Boian. 2002. The Rutgers Master II-new design force-feedback glove. *IEEE/ASME Transactions on mechatronics* 7, 2 (2002), 256–263.

[9] Caroline G.L. Cao, Mi Zhou, Daniel B. Jones, and Steven D. Schwaitzberg. 2007. Can Surgeons Think and Operate with Haptics at the Same Time? *Journal of Gastrointestinal Surgery* 11, 11 (2007), 1564–1569. https://doi.org/10.1007/s11605-007-0279-8

[10] Manuela Chessa, Guido Maiello, Lina K Klein, Vivian C Paulun, and Fabio Solari. 2019. Grasping objects in immersive Virtual Reality. In *2019 IEEE Conference on Virtual Reality and 3D User Interfaces (VR).* 1749–1754. https://doi.org/10.1109/VR.2019.8798155

[11] Francesco Chinello, Monica Malvezzi, Claudio Pacchierotti, and Domenico Prattichizzo. 2015. Design and development of a 3RRS wearable fingertip cutaneous device. In *2015 IEEE International Conference on Advanced Intelligent Mechatronics (AIM).* 293–298. https://doi.org/10.1109/AIM.2015.7222547

[12] Inrak Choi, Nick Corson, Lizzie Peiros, Elliot W Hawkes, Sean Keller, and Sean Follmer. 2017. A soft, controllable, high force density linear brake utilizing layer jamming. *IEEE Robotics and Automation Letters* 3, 1 (2017), 450–457.

[13] Inrak Choi, Heather Culbertson, Mark R. Miller, Alex Olwal, and Sean Follmer. 2017. Grabity: A Wearable Haptic Interface for Simulating Weight and Grasping in Virtual Reality. In *Proceedings of the 30th Annual ACM Symposium on User Interface Software and Technology* (Qubec City, Canada) *(UIST '17).* Association for Computing Machinery, New York, NY, USA, 119–130. https://doi.org/10.1145/3126594.3126599

[14] Lauri Connelly, Yicheng Jia, Maria L Toro, Mary Ellen Stoykov, Robert V Kenyon, and Derek G Kamper. 2010. A pneumatic glove and immersive virtual reality environment for hand rehabilitative training after stroke. *IEEE Transactions on Neural Systems and Rehabilitation Engineering* 18, 5 (2010), 551–559.

[15] Heather Culbertson, Juan José López Delgado, and Katherine J Kuchenbecker. 2014. One hundred data-driven haptic texture models and open-source methods for rendering on 3D objects. In *2014 IEEE haptics symposium (HAPTICS).* IEEE, 319–325.

[16] Swagata Das, Yusuke Kishishita, Toshio Tsuji, Cassie Lowell, Kazunori Ogawa, and Yuichi Kurita. 2018. ForceHand glove: A wearable force-feedback glove with pneumatic artificial muscles (PAMs). *IEEE Robotics and Automation Letters* 3, 3 (2018), 2416–2423.

[17] Stuart Diller, Carmel Majidi, and Steven H. Collins. 2016. A lightweight, low-power electroadhesive clutch and spring for exoskeleton actuation. In *2016 IEEE International Conference on Robotics and Automation (ICRA).* 682–689. https://doi.org/10.1109/ICRA.2016.7487194

[18] Stuart B Diller, Steven H Collins, and Carmel Majidi. 2018. The effects of electroadhesive clutch design parameters on performance characteristics. *Journal of Intelligent Material Systems and Structures* 29, 19 (2018), 3804–3828. https://doi.org/10.1177/1045389X18799474 arXiv:https://doi.org/10.1177/1045389X18799474

[19] Force Dimension. 2024. delta.3. Retrieved May 1, 2024 from https://www.forcedimension.com/products/delta.

[20] JD Edwards, BV Jayawant, WRC Dawson, and DT Wright. 1999. Permanent-magnet linear eddy-current brake with a non-magnetic reaction plate. *IEE Proceedings-Electric Power Applications* 146, 6 (1999), 627–631.

[21] Cathy Fang, Yang Zhang, Matthew Dworman, and Chris Harrison. 2020. Wireality: Enabling complex tangible geometries in virtual reality with worn multi-string haptics. In *Proceedings of the 2020 CHI Conference on Human Factors in Computing Systems.* 1–10.

[22] Likun Fang, Timo Müller, Erik Pescara, Nikola Fischer, Yiran Huang, and Michael Beigl. 2023. Investigating Passive Haptic Learning of Piano Songs Using Three Tactile Sensations of Vibration, Stroking and Tapping. *Proceedings of the ACM on Interactive, Mobile, Wearable and Ubiquitous Technologies* 7, 3 (2023), 1–19.

[23] Massimiliano Gabardi, Massimiliano Solazzi, Daniele Leonardis, and Antonio Frisoli. 2016. A new wearable fingertip haptic interface for the rendering of virtual shapes and surface features. In *2016 IEEE Haptics Symposium (HAPTICS).* 140–146. https://doi.org/10.1109/HAPTICS.2016.7463168

[24] Enrique Gallegos-Nieto, Hugo I. Medellín-Castillo, Germánico González-Badillo, Theodore Lim, and James Ritchie. 2017. The analysis and evaluation of the influence of haptic-enabled virtual assembly training on real assembly performance. *The International Journal of Advanced Manufacturing Technology* 89, 1 (2017), 581–598. https://doi.org/10.1007/s00170-016-9120-4

[25] Eric J Gonzalez, Eyal Ofek, Mar Gonzalez-Franco, and Mike Sinclair. 2021. X-rings: A hand-mounted 360 shape display for grasping in virtual reality. In *The 34th Annual ACM Symposium on User Interface Software and Technology.* 732–742.

[26] S. Grimnes. 1983. Dielectric breakdown of human skinin vivo. *Medical and Biological Engineering and Computing* 21, 3 (01 May 1983), 379–381. https://doi.org/10.1007/BF02478510

[27] Xiaochi Gu, Yifei Zhang, Weize Sun, Yuanzhe Bian, Dao Zhou, and Per Ola Kristensson. 2016. Dexmo: An Inexpensive and Lightweight Mechanical Exoskeleton for Motion Capture and Force Feedback in VR. In *Proceedings of the 2016 CHI Conference on Human Factors in Computing Systems* (San Jose, California, USA) *(CHI '16).* Association for Computing Machinery, New York, NY, USA, 1991–1995. https://doi.org/10.1145/2858036.2858487

[28] HaptX. 2023. HaptX. Retrieved May 1, 2024 from https://haptx.com/.

[29] Ronan Hinchet and Herbert Shea. 2019. High Force Density Textile Electrostatic Clutch. *Advanced Materials Technologies* 5, 4 (2019). https://doi.org/10.1002/admt.201900895

[30] Ronan Hinchet, Velko Vechev, Herbert Shea, and Otmar Hilliges. 2018. DextrES: Wearable Haptic Feedback for Grasping in VR via a Thin Form-Factor Electrostatic Brake. In *Proceedings of the 31st Annual ACM Symposium on User Interface Software and Technology* (Berlin,Germany) *(UIST '18)*. Association for Computing Machinery, New York, NY, USA, 901–912. https://doi.org/10.1145/3242587.3242657

[31] Ronan J. Hinchet and Herbert Shea. 2022. Glove- and Sleeve-Format Variable-Friction Electrostatic Clutches for Kinesthetic Haptics. *Advanced Intelligent Systems* 4, 12 (2022), 2200174. https://doi.org/10.1002/aisy.202200174 arXiv:https://onlinelibrary.wiley.com/doi/pdf/10.1002/aisy.202200174

[32] Matthias Hoppe, Beat Rossmy, Daniel Peter Neumann, Stephan Streuber, Albrecht Schmidt, and Tonja-Katrin Machulla. 2020. A human touch: Social touch increases the perceived human-likeness of agents in virtual reality. In *Proceedings of the 2020 CHI conference on human factors in computing systems*. 1–11.

[33] Mohssen Hosseini, Ali Sengül, Yudha Pane, Joris De Schutter, and Herman Bruyninck. 2018. ExoTen-Glove: A Force-Feedback Haptic Glove Based on Twisted String Actuation System. In *2018 27th IEEE International Symposium on Robot and Human Interactive Communication (RO-MAN)*. 320–327. https://doi.org/10.1109/ROMAN.2018.8525637

[34] Gunnar Jansson and Linda Monaci. 2006. Identification of real objects under conditions similar to those in haptic displays: providing spatially distributed information at the contact areas is more important than increasing the number of areas. *Virtual Reality* 9 (2006), 243–249.

[35] Minjae Jo, Dongkyu Kwak, and Sang Ho Yoon. 2023. WriMouCon: Wrist-Mounted Haptic Controller for Rendering Physical Properties in Virtual Reality. In *2023 IEEE World Haptics Conference (WHC)*. IEEE, 34–40.

[36] RS Johansson and AB Vallbo. 1979. Detection of tactile stimuli. Thresholds of afferent units related to psychophysical thresholds in the human hand. *The Journal of physiology* 297, 1 (1979), 405–422.

[37] Mirela Kahrimanovic, Wouter M. Bergmann Tiest, and Astrid M. L. Kappers. 2011. Discrimination thresholds for haptic perception of volume, surface area, and weight. *Attention, Perception, & Psychophysics* 73, 8 (01 Nov 2011), 2649–2656. https://doi.org/10.3758/s13414-011-0202-y

[38] Michinari Kono, Takumi Takahashi, Hiromi Nakamura, Takashi Miyaki, and Jun Rekimoto. 2018. Design Guideline for Developing Safe Systems that Apply Electricity to the Human Body. *ACM Trans. Comput.-Hum. Interact.* 25, 3, Article 19 (jun 2018), 36 pages. https://doi.org/10.1145/3184743

[39] Lik Hang Lee, Kit Yung Lam, Tong Li, Tristan Braud, Xiang Su, and Pan Hui. 2019. Quadmetric optimized thumb-to-finger interaction for force assisted one-handed text entry on mobile headsets. *Proceedings of the ACM on Interactive, Mobile, Wearable and Ubiquitous Technologies* 3, 3 (2019), 1–27.

[40] Mark J Lelieveld and Takashi Maeno. 2006. Design and development of a 4 DOF portable haptic interface with multi-point passive force feedback for the index finger. In *Proceedings 2006 IEEE International Conference on Robotics and Automation, 2006. ICRA 2006.* IEEE, 3134–3139.

[41] Yixuan Lin, Yuqiong Zhang, Fan Zhang, Meining Zhang, Dalong Li, Gaofeng Deng, Li Guan, and Mingdong Dong. 2021. Studies on the electrostatic effects of stretched PVDF films and nanofibers. *Nanoscale Research Letters* 16, 1 (03 May 2021), 79. https://doi.org/10.1186/s11671-021-03536-9

[42] Abhijeet Mishra, Piyush Kumar, Jainendra Shukla, and Aman Parnami. 2022. HaptiDrag: A device with the ability to generate varying levels of drag (friction) effects on real surfaces. *Proceedings of the ACM on Interactive, Mobile, Wearable and Ubiquitous Technologies* 6, 3 (2022), 1–26.

[43] Takuro Nakao, Kai Kunze, Megumi Isogai, Shinya Shimizu, and Yun Suen Pai. 2020. Fingerflex: Shape memory alloy-based actuation on fingers for kinesthetic haptic feedback. *19th International Conference on Mobile and Ubiquitous Multimedia* (2020). https://doi.org/10.1145/3428361.3428404

[44] Romain Nith, Shan-Yuan Teng, Pengyu Li, Yujie Tao, and Pedro Lopes. 2021. DextrEMS: Increasing dexterity in electrical muscle stimulation by combining it with brakes. In *The 34th annual ACM symposium on user interface software and technology*. 414–430.

[45] Wataru Nozaki, Ken'ichi Koyanagi, Toru Oshima, Takayuki Matsuno, and Noboru Momose. 2007. Development of passive force display glove system and its improved mechanism. In *2007 International Conference on Mechatronics and Automation*. IEEE, 2645–2650.

[46] Claudio Pacchierotti, Stephen Sinclair, Massimiliano Solazzi, Antonio Frisoli, Vincent Hayward, and Domenico Prattichizzo. 2017. Wearable haptic systems for the fingertip and the hand: taxonomy, review, and perspectives. *IEEE transactions on haptics* 10, 4 (2017), 580–600.

[47] Sungjune Park, Jun Shintake, Yegor Piskarev, Yuwen Wei, Ishan Joshipura, Ethan Frey, Taylor Neumann, Dario Floreano, and Michael D Dickey. 2021. Stretchable and Soft Electroadhesion Using Liquid-Metal Subsurface Microelectrodes. *Advanced Materials Technologies* 6, 9 (2021), 2100263.

[48] Evan Pezent, Ali Israr, Majed Samad, Shea Robinson, Priyanshu Agarwal, Hrvoje Benko, and Nick Colonnese. 2019. Tasbi: Multisensory squeeze and vibrotactile wrist haptics for augmented and virtual reality. In *2019 IEEE World Haptics Conference (WHC)*. IEEE, 1–6.

[49] Project Peta pico Voltron. [n. d.]. SHVPS Single Channel High Voltage Power Supply. Retrieved May 1, 2024 from https://petapicovoltron.com/single-channel-high-voltage-power-supply.

[50] Harsha Prahlad, Ron Pelrine, Scott Stanford, John Marlow, and Roy Kornbluh. 2008. Electroadhesive robots—wall climbing robots enabled by a novel, robust, and electrically controllable adhesion technology. In *2008 IEEE international conference on robotics and automation*. IEEE, 3028–3033.

[51] Pornthep Preechayasomboon and Eric Rombokas. 2021. Haplets: Finger-Worn Wireless and Low-Encumbrance Vibrotactile Haptic Feedback for Virtual and Augmented Reality. *Frontiers in Virtual Reality* 2 (2021). https://doi.org/10.3389/frvir.2021.738613

[52] Jiaming Qi, Feng Gao, Guanghui Sun, Joo Chuan Yeo, and Chwee Teck Lim. 2023. HaptGlove—Untethered Pneumatic Glove for Multimode Haptic Feedback in Reality–Virtuality Continuum. *Advanced Science* 10, 25 (2023), 2301044. https://doi.org/10.1002/advs.202301044 arXiv:https://onlinelibrary.wiley.com/doi/pdf/10.1002/advs.202301044

[53] Vivek Ramachandran, Jun Shintake, and Dario Floreano. 2019. All-fabric wearable electroadhesive clutch. *Advanced Materials Technologies* 4, 2 (2019), 1800313.

[54] R. Ranjithkumar, J. Deepak Rosario, Rajesh Swaminathan, Nandhakumar Raju, Vidhya Bhojan, and Sakunthala Ayyasamy. 2023. Improved load bearing performance of electroadhesive tapes with Hexagonal boron nitride/Barium titanate composite in Poly (vinylidene fluoride co-hexafluoropropylene). *Journal of Materials Science: Materials in Electronics* 34, 4 (2023), 308. https://doi.org/10.1007/s10854-022-09543-5

[55] Gabriel Robles-De-La-Torre and Vincent Hayward. 2001. Force can overcome object geometry in the perception of shape through active touch. *Nature* 412, 6845 (2001), 445–448.

[56] Ioannis Sarakoglou, Anais Brygo, Dario Mazzanti, Nadia Garcia Hernandez, Darwin G Caldwell, and Nikos G Tsagarakis. 2016. Hexotrac: A highly under-actuated hand exoskeleton for finger tracking and force feedback. In *2016 IEEE/RSJ International Conference on Intelligent Robots and Systems (IROS)*. IEEE, 1033–1040.

[57] Suji Sathiyamurthy, Melody Lui, Erin Kim, and Oliver Schneider. 2021. Measuring Haptic Experience: Elaborating the HX model with scale development. In *2021 IEEE World Haptics Conference (WHC)*. IEEE, 979–984.

[58] Emanuele Lindo Secco and Andualem Maereg Tadesse. 2020. A Wearable Exoskeleton for Hand Kinesthetic Feedback in Virtual Reality. In *Wireless Mobile Communication and Healthcare*, Gregory M.P. O'Hare, Michael J. O'Grady, John O'Donoghue, and Patrick Henn (Eds.). Springer International Publishing, Cham, 186–200.

[59] Vivian Shen, Tucker Rae-Grant, Joe Mullenbach, Chris Harrison, and Craig Shultz. 2023. Fluid Reality: High-Resolution, Untethered Haptic Gloves using Electroosmotic Pump Arrays. In *Proceedings of the 36th Annual ACM Symposium on User Interface Software and Technology*. 1–20.

[60] Alejandro Jarillo Silva, Omar A. Domínguez Ramirez, Vicente Parra Vega, and Jesus P. Ordaz Oliver. 2009. PHANToM OMNI Haptic Device: Kinematic and Manipulability. In *2009 Electronics, Robotics and Automotive Mechanics Conference (CERMA)*. 193–198. https://doi.org/10.1109/CERMA.2009.55

[61] Bukun Son and Jaeyoung Park. 2018. Haptic feedback to the palm and fingers for improved tactile perception of large objects. In *Proceedings of the 31st Annual ACM Symposium on User Interface Software and Technology*. 757–763.

[62] Kahye Song, Sung Hee Kim, Sungho Jin, Sohyun Kim, Sunho Lee, Jun-Sik Kim, Jung-Min Park, and Youngsu Cha. 2019. Pneumatic actuator and flexible piezoelectric sensor for soft virtual reality glove system. *Scientific Reports* 9, 1 (18 Jul 2019), 8988. https://doi.org/10.1038/s41598-019-45422-6

[63] Hong Z. Tan, Mandayam A. Srinivasan, Charlotte M. Reed, and Nathaniel I. Durlach. 2007. Discrimination and identification of finger joint-angle position using active motion. *ACM Trans. Appl. Percept.* 4, 2 (jul 2007), 10–es. https://doi.org/10.1145/1265957.1265959

[64] Novint Technologies. 2024. Novint Falcon. Retrieved May 1, 2024 from https://hapticshouse.com/pages/novints-falcon-haptic-device.

[65] Shan-Yuan Teng, Pengyu Li, Romain Nith, Joshua Fonseca, and Pedro Lopes. 2021. Touch&fold: A foldable haptic actuator for rendering touch in mixed reality. In *Proceedings of the 2021 CHI Conference on Human Factors in Computing Systems*. 1–14.

[66] Roshan Thilakarathna and Maroay Phlernjai. 2024. Design and development of a lightweight, low-cost cylindrical electrostatic clutch. *Engineering Science and Technology, an International Journal* 49 (2024), 101600.

[67] Qianqian Tong, Wenxuan Wei, Yuru Zhang, Jing Xiao, and Dangxiao Wang. 2023. Survey on hand-based haptic interaction for virtual reality. *IEEE Transactions on Haptics* (2023).

[68] Eleftherios Triantafyllidis, Christopher Mcgreavy, Jiacheng Gu, and Zhibin Li. 2020. Study of Multimodal Interfaces and the Improvements on Teleoperation. *IEEE Access* 8 (2020), 78213–78227. https://doi.org/10.1109/ACCESS.2020.2990080

[69] Dzmitry Tsetserukou, Shotaro Hosokawa, and Kazuhiko Terashima. 2014. LinkTouch: A wearable haptic device with five-bar linkage mechanism for presentation of two-DOF force feedback at the fingerpad. In *2014 IEEE Haptics Symposium (HAPTICS)*. 307–312. https://doi.org/10.1109/HAPTICS.2014.6775473

[70] C.S. Tzafestas. 2003. Whole-hand kinesthetic feedback and haptic perception in dextrous virtual manipulation. *IEEE Transactions on Systems, Man, and Cybernetics - Part A: Systems and Humans* 33, 1 (2003), 100–113. https://doi.org/10.1109/TSMCA.2003.812600

[71] Yusuke Ujitoko, Takaaki Taniguchi, Sho Sakurai, and Koichi Hirota. 2020. Development of Finger-Mounted High-Density Pin-Array Haptic Display. *IEEE Access* 8 (2020), 145107–145114. https://doi.org/10.1109/ACCESS.2020.3015058

[72] Nicha Vanichvoranun and Sang Ho Yoon. 2023. A Lightweight Wearable Multi-joint Force Feedback for High Definition Grasping in VR. In *2023 IEEE Conference on Virtual Reality and 3D User Interfaces Abstracts and Workshops (VRW)*. 625–626. https://doi.org/10.1109/

VRW58643.2023.00155

[73] Velko Vechev, Ronan Hinchet, Stelian Coros, Bernhard Thomaszewski, and Otmar Hilliges. 2022. Computational Design of Active Kinesthetic Garments. In *Proceedings of the 35th Annual ACM Symposium on User Interface Software and Technology*. 1–11.

[74] Velko Vechev, Juan Zarate, David Lindlbauer, Ronan Hinchet, Herbert Shea, and Otmar Hilliges. 2019. Tactiles: Dual-mode low-power electromagnetic actuators for rendering continuous contact and spatial haptic patterns in vr. In *2019 IEEE Conference on Virtual Reality and 3D User Interfaces (VR)*. IEEE, 312–320.

[75] Dangxiao Wang, Meng Song, Afzal Naqash, Yukai Zheng, Weiliang Xu, and Yuru Zhang. 2018. Toward whole-hand kinesthetic feedback: A survey of force feedback gloves. *IEEE transactions on haptics* 12, 2 (2018), 189–204.

[76] Eric Whitmire, Hrvoje Benko, Christian Holz, Eyal Ofek, and Mike Sinclair. 2018. Haptic revolver: Touch, shear, texture, and shape rendering on a reconfigurable virtual reality controller. In *Proceedings of the 2018 CHI conference on human factors in computing systems*. 1–12. https://doi.org/10.1145/3173574.3173660

[77] Scott H Winter and Mourad Bouzit. 2007. Use of magnetorheological fluid in a force feedback glove. *IEEE Transactions on Neural Systems and Rehabilitation Engineering* 15, 1 (2007), 2–8.

[78] Quan Xiong, Xuanquan Liang, Daiyue Wei, Huacen Wang, Renjie Zhu, Ting Wang, Jianjun Mao, and Hongqiang Wang. 2022. So-EAGlove: VR haptic glove rendering softness sensation with force-tunable electrostatic adhesive brakes. *IEEE Transactions on Robotics* 38, 6 (2022), 3450–3462.

[79] Y. Yokokohji, R.L. Hollis, and T. Kanade. 1996. What you can see is what you can feel-development of a visual/haptic interface to virtual environment. In *Proceedings of the IEEE 1996 Virtual Reality Annual International Symposium*. 46–53. https://doi.org/10.1109/VRAIS.1996.490509

[80] Shigeo Yoshida, Yuqian Sun, and Hideaki Kuzuoka. 2020. PoCoPo: Handheld Pin-based Shape Display for Haptic Rendering in Virtual Reality. In *Proceedings of the 2020 CHI Conference on Human Factors in Computing Systems* (Honolulu,USA) *(CHI '20)*. Association for Computing Machinery, New York, NY, USA, 1–13. https://doi.org/10.1145/3313831.3376358

[81] Zhilin Zhang, Chunlin Li, Jian Zhang, Qiang Huang, Ritsu Go, Tianyi Yan, and Jinglong Wu. 2018. Discrimination threshold for haptic volume perception of fingers and phalanges. *Attention, Perception, & Psychophysics* 80, 2 (01 Feb 2018), 576–585. https://doi.org/10.3758/s13414-017-1453-z

A EXPLORATORY STUDY: HAPTIC RENDERING ALGORITHM

Algorithm 1 illustrates the overall haptic rendering pipeline of our method.

Algorithm 1 Actuation states update

Require: Status of each phalange
Ensure: Actuation states of DP, IP, and PP
  Set *DP*, *IP*, and *PP* to the current actuation states of DP, IP, and PP respectively ▷ IP status of thumb is always *False*
  while True **do**
    Set *DP* to DP status
    if DP status is *True* **then**
      Set *PP* to *False*
      Set *IP* to IP status AND PP status ▷ When DP state is *True*, PP is *True* only when its state and PP state is *True*
    else
      Set *IP* to IP status
      if IP status is *False* **then**
        Set *PP* to PP status
      end if
    end if
  end while

B USER STUDY CONFUSION MATRIX

Figure 16~18 show confusion matrices from our User Study 1.

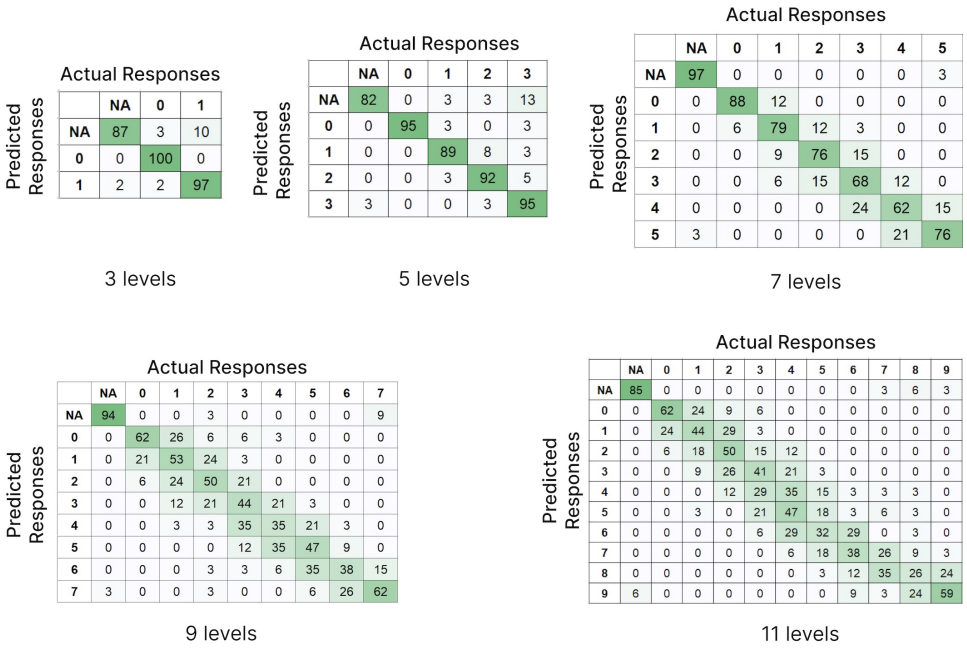

Fig. 17. Confusion matrix of task1: Bending all phalanges with All-Phalange Activation

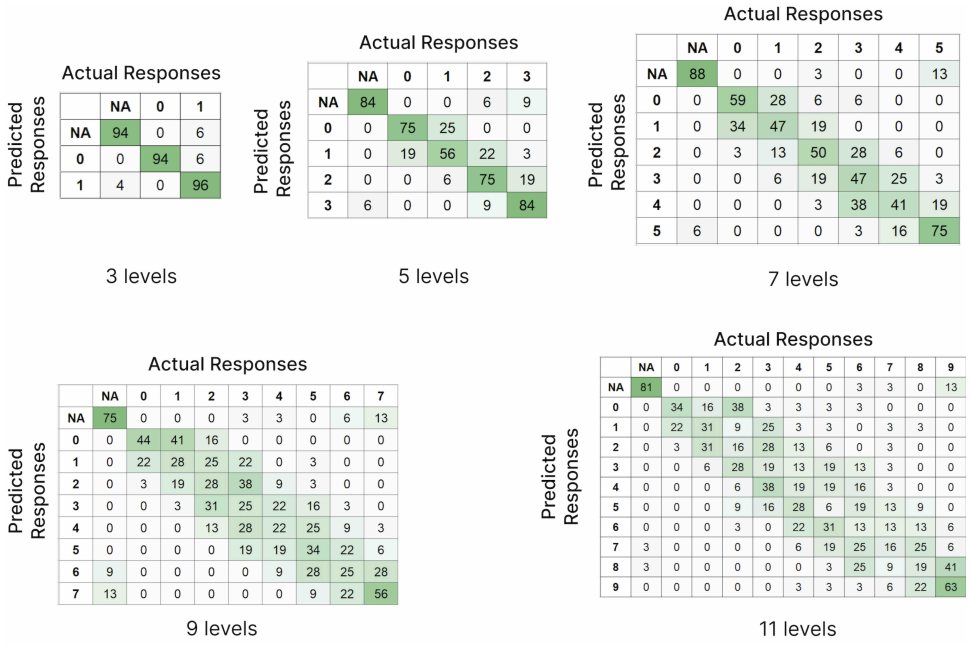

Fig. 18. Confusion matrix of task1: Bending all phalanges with DP only Activation

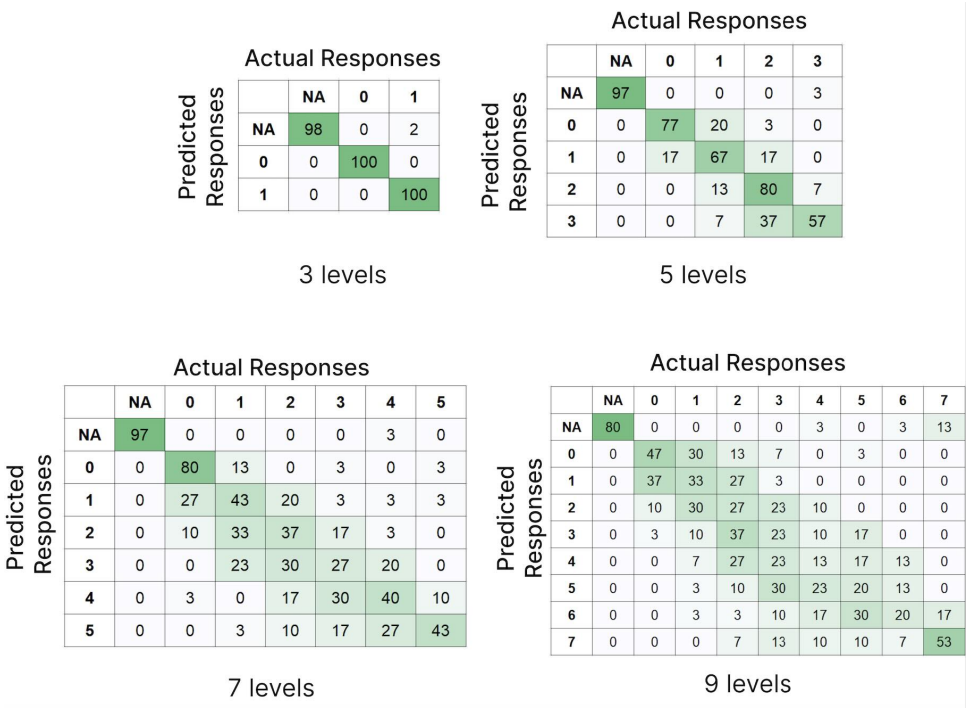

Fig. 19. Confusion matrix of task: Bending DP + IP